

A Systematic Study on Weak Galerkin Finite Element Method for Second Order Parabolic Problems

Bhupen Deka* and Naresh Kumar†

Abstract

A systematic numerical study on weak Galerkin (WG) finite element method for second order linear parabolic problems is presented by allowing polynomial approximations with various degrees for each local element. Convergence of both semidiscrete and fully discrete WG solutions are established in $L^\infty(L^2)$ and $L^\infty(H^1)$ norms for a general WG element $(\mathcal{P}_k(K), \mathcal{P}_j(\partial K), [\mathcal{P}_l(K)]^2)$, where $k \geq 1$, $j \geq 0$ and $l \geq 0$ are arbitrary integers. The fully discrete space-time discretization is based on a first order in time Euler scheme. Our results are intended to extend the numerical analysis of WG methods for elliptic problems [J. Sci. Comput., 74 (2018), 1369-1396] to parabolic problems. Numerical experiments are reported to justify the robustness, reliability and accuracy of the WG finite element method.

Key words. Parabolic problems, weak Galerkin finite element method, discrete weak gradient, semidiscrete and fully discrete schemes, convergence analysis.

AMS Subject Classifications(2010). 65N15, 65N30.

1 Introduction

We consider the following linear parabolic equation of the form

$$u_t - \nabla \cdot (a \nabla u) = f \quad \text{in } \Omega \times (0, T] \quad (1.1)$$

with initial and boundary conditions

$$u(x, 0) = \psi(x) \quad \text{in } \Omega; \quad u = 0 \quad \text{on } \partial\Omega \times (0, T], \quad (1.2)$$

where $\Omega \subset \mathbb{R}^2$ is a bounded domain with smooth boundary $\partial\Omega$. We assume that the coefficient matrix $a = (a_{ij}(x))_{2 \times 2} \in [L^\infty(\Omega)]^{2^2}$ is symmetric and uniformly positive definite in Ω . The initial function $\psi = \psi(x)$ and the forcing function $f = f(x, t)$ are assumed to be smooth functions in their respective domains of definition, and T is the finite terminal observation time.

Finite element approximations of linear parabolic equations have been studied extensively, [33] contains a comprehensive list of references. Recently, the weak Galerkin finite element method has attracted much attention in the field of numerical partial differential equations. The objective of the present work is

*Department of Mathematics, Indian Institute of Technology Guwahati, Guwahati - 781039, India (bdeka@iitg.ac.in).

†Department of Mathematics, Indian Institute of Technology Guwahati, Guwahati - 781039, India (naresh176123101@iitg.ac.in).

to propose a systematic framework for the weak Galerkin finite element method (WG-FEM for short) for second order linear parabolic equations by using polynomials of various degrees in the weak finite element space. The WG-FEM introduced in [38] refers to the numerical algorithms for differential equations where the differential operators appearing in the variational forms are to project into another appropriately chosen Sobolev space such that its approximation by polynomials is possible. More precisely, the WG finite element approximations are derived from the weak formulations of the problems by replacing differential operators involved by its weak forms and adding parameter free stabilizers. In fact, WG formulation is a natural extension of conforming finite element formulation when nonconforming elements are used. The concept of weak derivatives makes WG a widely applicable numerical technique for a large variety of PDEs arising from the mathematical modeling of practical problems in science and engineering. There is an abundant literature on such PDEs; see, e.g., elliptic equation [18, 20, 21, 22, 27, 36, 37, 39], parabolic equation [19, 42, 43, 45], system of equations [23, 25, 26, 28, 29, 31, 35, 40, 44], interface problems [17, 30, 32]. One close relative of the WG finite element method is the hybridizable discontinuous Galerkin (HDG) method [10]. But they make use of different polynomial approximating spaces and utilize different stabilization techniques. For detailed discussions, we refer to [8, 41].

The classical finite element methods based on conforming finite element discretization, have limitations in practical computation. The conforming finite element space is restricted to piecewise polynomials with prescribed continuity that ensures conformity and stability of the corresponding weak formulation, which is often very difficult to implement, particularly for problems in high dimensions and/or on general polytopal partitions. In scientific computing, higher order of convergence is always one of the major research goals, because high order methods are more accurate and cost efficient. Although conforming finite element methods have simple formulations with many fewer unknowns, construction of conforming finite element spaces of any orders would be either challenging or impossible. Keeping in mind the applicability of numerical methods of higher order with polygonal meshes, recently attempts have been made to develop certain technologies which make use of polygonal meshes, for instance, see [4, 11, 34] for virtual element methods, [3, 6, 7, 9, 10] for discontinuous Galerkin methods. Due to the use of discontinuous approximation functions, WG-FEMs are highly flexible in construction of finite element spaces of any orders with the price of more degrees of freedom and more complex formulations. Unlike classical finite element method, the WG-FEM is applicable for unstructured polygonal meshes making it more suitable for complex geometry usually appeared in real life problem. A typical local WG element is of the form $(\mathcal{P}_k(K), \mathcal{P}_j(\partial K), [\mathcal{P}_l(K)]^2)$, where $k \geq 1$ is the degree of polynomials in the interior of the element K , $j \geq 0$ is the degree of polynomials on the boundary of K , and $l \geq 0$ is the degree of polynomials employed in the computation of weak gradients or weak first order partial derivatives. The accuracy and the computational complexity of the corresponding WG scheme is significantly impacted by the selection of such polynomials. The goal of this study is to explore all possible combinations of polynomial functions in the reconstruction of the underlying differential operators. Our results are intended to extend the weak Galerkin analysis in [37] for elliptic problems to linear parabolic equations with polygonal meshes. More precisely, the analysis presented in this article shows that the WG finite element solutions approximate the true solutions with an optimal order in $L^\infty(L^2)$ and $L^\infty(H^1)$ norms. The results for parabolic equation are particularly useful because it demonstrate the robustness of the WG-FEMs

with various combinations of polynomials in the numerical scheme and it fills a gap in literature. It is worth to note that only H^1 norm error estimate is established in [37]. Finally, theoretical convergence results are validated for several combination of the polynomial spaces.

The rest of the paper is organized as follows. In Section 2, we introduce some commonly used notations. Further, we review the definitions of weak gradient and its discrete analogs in suitable polynomial spaces. Section 3 is devoted to the optimal order error estimates of semidiscrete WG-FEM algorithm. In Section 4, a backward Euler scheme is described along with a priori error bounds in $L^\infty(H^1)$ and $L^\infty(L^2)$ norms. Section 5 focuses on some numerical results that confirm the convergence theory developed in earlier section. Summary on the new results developed in this paper are presented in Section 6. Finally, in ‘‘Appendix’’ we present some detailed computational results leading to the reported rate of convergence for some typical combinations.

Throughout the paper, C is a positive generic constant independent of the mesh parameters $\{h, \tau\}$ and whose value changes with context.

2 Preliminaries and Weak Galerkin Discretization

2.1 Basic Notations

Let us introduce some notations used in this paper. In this work, we will follow the standard notation for Sobolev spaces and norms (cf. [2]). For a domain $\mathcal{K} \subseteq \Omega \subset \mathbb{R}^2$, non-negative integer m and real p ($1 \leq p \leq \infty$), $W^{m,p}(\mathcal{K})$ represents the standard Sobolev space (cf. [2]). For $p = 2$, we use $H^m(\mathcal{K})$ for $W^{m,2}(\mathcal{K})$ with inner product $(\cdot, \cdot)_{m,\mathcal{K}}$. Notations $\|\cdot\|_{m,\mathcal{K}}$ and $|\cdot|_{m,\mathcal{K}}$ are used to denote the norm and seminorm in the Sobolev space $H^m(\mathcal{K})$, respectively. Inner product in $H^m(\mathcal{K})$ is denoted by $(\cdot, \cdot)_{m,\mathcal{K}}$. Clearly, $H^0(\mathcal{K}) = L^2(\mathcal{K})$ with inner product $(\cdot, \cdot)_{\mathcal{K}}$ and induced norm $\|\cdot\|_{\mathcal{K}}$. For our convenience, we skip the subscript \mathcal{K} in the inner product notation and norm when $\mathcal{K} = \Omega$. $H_0^1(\Omega)$ is the collection of all $H^1(\Omega)$ functions vanishing on the boundary of Ω .

For a given Banach space $(\mathcal{B}, \|\cdot\|_{\mathcal{B}})$ and interval $J \subset \mathbb{R}$, we define for $m = 0, 1$,

$$H^m(J; \mathcal{B}) = \left(u(t) \in \mathcal{B} \text{ for a.e. } t \in J \text{ and } \sum_{j=0}^m \int_J \left\| \frac{\partial^j u(t)}{\partial t^j} \right\|_{\mathcal{B}}^2 dt < \infty \right)$$

endowed with the following norm

$$\|u\|_{H^m(J; \mathcal{B})} = \left(\sum_{j=0}^m \int_J \left\| \frac{\partial^j u(t)}{\partial t^j} \right\|_{\mathcal{B}}^2 dt \right)^{\frac{1}{2}}.$$

Further, $L^\infty(J; \mathcal{B})$ is also a Banach space with respect to following norm

$$\|\phi\|_{L^\infty(J; \mathcal{B})} := \text{ess} \sup_{t \in [0, T]} \|\phi(t)\|_{\mathcal{B}}.$$

For the simplicity, we use $L^2(\mathcal{B})$ for $L^2(J; \mathcal{B})$, $L^\infty(\mathcal{B})$ for $L^\infty(J; \mathcal{B})$ and $H^1(\mathcal{B})$ for $H^1(J; \mathcal{B})$.

We end this section with the following regularity result for the initial boundary value problem (1.1)-(1.2) (see, [24], p. 287, Theorem 2.10).

Theorem 2.1.1. *Assume that $f \in L^2(0, T; H^{r-1}(\Omega))$ and $\psi \in H^r(\Omega)$ for some $r \geq 1$. Then the solution of (1.1)-(1.2) satisfies*

$$u \in L^2(0, T; H^{r+1}(\Omega)) \cap H^1(0, T; H^{r-1}(\Omega)). \quad \square$$

2.2 Weak Galerkin Discretization

In this section, we shall describe the weak Galerkin finite element discretization for the problem (1.1)-(1.2) and review the definition of the weak gradient operator.

Let \mathcal{T}_h be a partition of the domain Ω consisting of polygons in two dimension satisfying a set of conditions specified in [37, 39]. Denote by \mathcal{E}_h the set of all edges in \mathcal{T}_h and let $\mathcal{E}_h^0 = \mathcal{E}_h \setminus \partial\Omega$ be the set of all interior edges. For every element $K \in \mathcal{T}_h$, we denote by $|K|$ the measure of K and by h_K its diameter and mesh size $h = \max_{K \in \mathcal{T}_h} h_K$ for \mathcal{T}_h .

The key in weak Galerkin methods is the use of weak derivatives in the place of strong derivatives in the variational form for the underlying partial differential equations. Thus, it is essential to introduce a weak version for the gradient operator. Weak gradient operators and its discrete version were introduced in [38, 39], and the rest of the section will review them. Let K be any polygonal domain with interior K^0 and boundary ∂K . A weak function on the region K refers to a pair of scalar valued functions $v = \{v_0, v_b\}$ such that $v_0 \in L^2(K)$ and $v_b \in L^2(\partial K)$. Denote by $\mathcal{V}(K)$ the space of weak scalar valued functions on K ; i.e.,

$$\mathcal{V}(K) = \{v = \{v_0, v_b\} : v_0 \in L^2(K), v_b \in L^2(\partial K)\}. \quad (2.1)$$

For any given integer $k \geq 0$, denote $\mathcal{P}_k(K)$ the space of polynomials of total degree k or less on the element $K \in \mathcal{T}_h$. Analogously, for any given integer $j \geq 0$, $\mathcal{P}_j(e)$ denotes the space of polynomials of total degree j or less on the edge $e \in \mathcal{E}_h$. On each element $K \in \mathcal{T}_h$, define the following local weak finite element space

$$\mathcal{V}(k, j, K) = \{v = \{v_0, v_b\} : v_0 \in \mathcal{P}_k(K), v_b \in \mathcal{P}_j(\partial K)\}. \quad (2.2)$$

A global weak finite element space \mathcal{V}_h is constructed by patching local space $\mathcal{V}(k, j, K)$ through a common value of v_b on all interior edges

$$\mathcal{V}_h = \{v = \{v_0, v_b\} : v|_K \in \mathcal{V}(k, j, K), [v]_e = 0, \forall e \in \mathcal{E}_h^0\}. \quad (2.3)$$

Here, $[v]_e$ denotes the jump of $v \in \mathcal{V} = \prod_{K \in \mathcal{T}_h} \mathcal{V}(k, j, K)$ across an interior edge $e \in \mathcal{E}_h^0$. Denote by \mathcal{V}_h^0 the subspace of \mathcal{V}_h consisting of all finite element functions with vanishing boundary value

$$\mathcal{V}_h^0 = \{v \in \mathcal{V}_h : v_b|_{\partial\Omega} = 0\}. \quad (2.4)$$

Next, we introduce a discrete weak gradient operator, denoted by ∇_w , is defined as the unique polynomial $(\nabla_w v) \in [\mathcal{P}_l(K)]^2$ that satisfies the following equation

$$(\nabla_w v, \phi)_K = - \int_K v_0 (\nabla \cdot \phi) dK + \int_{\partial K} v_b (\phi \cdot \mathbf{n}) ds \quad \forall \phi \in [\mathcal{P}_l(K)]^2. \quad (2.5)$$

where \mathbf{n} is the outward normal to ∂K and $l \geq 0$ is prescribed non-negative integer. By applying the divergence theorem to the first term on the right-hand side of (2.5) we arrive at

$$(\nabla_w v, \phi)_K = (\nabla v_0, \phi)_K + \langle v_b - v_0, \phi \cdot \mathbf{n} \rangle_{\partial K} \quad \forall \phi \in [\mathcal{P}_l(K)]^2. \quad (2.6)$$

Using the discrete weak gradient operator ∇_w , we define a bilinear map $\mathcal{A} : \mathcal{V}_h \times \mathcal{V}_h \rightarrow \mathbb{R}$ by

$$\mathcal{A}(u_h, v_h) = \sum_{K \in \mathcal{T}_h} (a \nabla_w u_h, \nabla_w v_h)_K + \mathcal{S}(u_h, v_h) \quad \forall u_h, v_h \in \mathcal{V}_h. \quad (2.7)$$

Here, $\mathcal{S}(\cdot, \cdot)$ is known as stabilizer, which is a semi-positive definite bilinear form defined on $\mathcal{V}_h \times \mathcal{V}_h$. Stabilizer $\mathcal{S}(\cdot, \cdot)$ is often chosen in such a way that it fits well into the theory and implementation of the WG numerical scheme. For examples (cf. [37]):

Example 2.1. (*Projected Element-Boundary Discrepancy*) For $v_h = \{v_0, v_b\} \in \mathcal{V}_h$, the continuity of v_h can be measured by the quantity $v_b - v_0|_{\partial K}$ for each element $K \in \mathcal{T}_h$. The projected element-boundary-discrepancy method is based on the following stabilizer

$$\mathcal{S}(u_h, v_h) = \sum_{K \in \mathcal{T}_h} h_K^{-1} \langle \mathcal{Q}_m(u_b - u_0|_{\partial K}), \mathcal{Q}_m(v_b - v_0|_{\partial K}) \rangle_{\partial K}, \quad (2.8)$$

where $\mathcal{Q}_m : L^2(\partial K) \rightarrow \mathcal{P}_m(\partial K)$ is the usual L^2 -projection operator and $m = \max\{j, l\}$.

Example 2.2. (*Element-Boundary Discrepancy*) The element-boundary-discrepancy method is based on the following stabilizer

$$\mathcal{S}(u_h, v_h) = \sum_{K \in \mathcal{T}_h} h_K^{-1} \langle u_b - u_0|_{\partial K}, v_b - v_0|_{\partial K} \rangle_{\partial K}. \quad (2.9)$$

In the WG methods, the polynomial degree and the stabilizer must be chosen so that the bilinear form $\mathcal{A}(\cdot, \cdot)$ is coercive with respect to the semi-norm $\|\cdot\|_{1,h}$ (cf. [37]) defined by

$$\|v_h\|_{1,h} = \left(\sum_{K \in \mathcal{T}_h} (\|\nabla v_0\|_K^2 + h_K^{-1} \|v_0 - v_b\|_{\partial K}^2) \right)^{\frac{1}{2}}, \quad v_h = \{v_0, v_b\} \in \mathcal{V}_h. \quad (2.10)$$

More precisely, there exist constants $C_1, C_2 > 0$ such that for any $v_h \in \mathcal{V}_h$, the following inequality holds true

$$C_1 \|v_h\|_{1,h}^2 \leq \mathcal{A}(v_h, v_h) \leq C_2 \|v_h\|_{1,h}^2. \quad (2.11)$$

The coercivity inequality (2.11), for both the stabilizers on weak Galerkin space $(\mathcal{P}_k(K), \mathcal{P}_j(\partial K), [\mathcal{P}_l(K)]^2)$, is stated below (cf. [37]).

Lemma 2.1. Assume that $l \geq k - 1$ and $m = \max\{j, l\}$. Then the coercivity inequality (2.11) holds true.

We end this section with some standard L^2 projections. For each element $K \in \mathcal{T}_h$ and edge $e \in \mathcal{E}_h$, operators $\mathcal{Q}_k^0 : L^2(K) \rightarrow \mathcal{P}_k(K)$ and $\mathcal{Q}_j^b : L^2(e) \rightarrow \mathcal{P}_j(e)$ are the usual L^2 projections. Denote by \mathcal{Q}_h the L^2 projection onto the finite element space \mathcal{V}_h such that $\mathcal{Q}_h|_K = \{\mathcal{Q}_k^0, \mathcal{Q}_j^b\}$. In addition to \mathcal{Q}_h , let $\mathcal{Q}_l : [L^2(K)]^2 \rightarrow [\mathcal{P}_l(K)]^2$ be an another local L^2 projection.

3 Error analysis for the semidiscrete scheme

This section deals with the error analysis for the spatially discrete scheme. Optimal order of convergence in both $L^\infty(L^2)$ and $L^\infty(H^1)$ norms are established.

A time-dependent weak function $v_h : [0, T] \rightarrow \mathcal{V}_h$ is written as $v_h(t) := \{v_0(t), v_b(t)\}$ and subsequently we define $v_{ht}(t) := \{v'_0(t), v'_b(t)\}$, where ‘ \prime ’ denotes the time derivatives. For simplicity, we use $v_h = \{v_0, v_b\}$ for $v_h(t)$ and $v_{ht} = \{v'_0, v'_b\}$ for $v_{ht}(t)$.

The continuous-time weak Galerkin finite element approximation to (1.1)-(1.2) can be obtained by seeking $u_h = \{u_0, u_b\} : [0, T] \rightarrow \mathcal{V}_h^0$ satisfying following equation

$$(u_{ht}, v_0) + \mathcal{A}(u_h, v_h) = (f, v_0) \quad \forall v_h \in \mathcal{V}_h^0, \quad (3.1)$$

where $u_h(0) \in \mathcal{V}_h^0$ is a suitable approximation of the initial function ψ . Well-posedness of the scheme (3.1) can be verified from the fact that weak finite element space \mathcal{V}_h^0 is a normed linear space with respect to the triple norm $\|\cdot\|$ defined as

$$\|v_h\| = \sqrt{\mathcal{A}(v_h, v_h)}, \quad v_h \in \mathcal{V}_h^0.$$

As a standard procedure in finite element method, we split our error into two components using an intermediate operator. We write

$$u - u_h = (u - \mathcal{Q}_h u) + (\mathcal{Q}_h u - u_h).$$

For simplicity, we introduce the following notation

$$e_h(t) := \{e_0(t), e_b(t)\} = u_h(t) - \mathcal{Q}_h u(t), \quad t \in [0, T]. \quad (3.2)$$

Then e_h satisfies following error equation which is crucial for our later analysis.

Lemma 3.1. *Let e_h be the error as defined in (3.2). Then, for all $v_h = \{v_0, v_b\} \in \mathcal{V}_h^0$, we have*

$$(e_{ht}, v_0) + \mathcal{A}(e_h, v_h) = l_1(u, v_h) + l_2(u, v_h) + l_3(u, v_h) + \mathcal{S}(\mathcal{Q}_h u, v_h), \quad (3.3)$$

where bilinear forms $l_1(\cdot, \cdot)$, $l_2(\cdot, \cdot)$ and $l_3(\cdot, \cdot)$ are given by

$$\begin{aligned} l_1(u, v_h) &= \sum_{K \in \mathcal{T}_h} \left(\mathcal{Q}_l(a \mathcal{Q}_l \nabla \mathcal{Q}_k^0 u) - a \nabla u, \nabla v_0 \right)_K, \\ l_2(u, v_h) &= \sum_{K \in \mathcal{T}_h} \langle (\mathcal{Q}_l(a \mathcal{Q}_l \nabla \mathcal{Q}_k^0 u) - a \nabla u) \cdot \mathbf{n}, v_b - v_0 \rangle_{\partial K}, \\ l_3(u, v_h) &= \sum_{K \in \mathcal{T}_h} \langle \mathcal{Q}_j^b u - \mathcal{Q}_k^0 u, \mathcal{Q}_l(a \nabla_w v) \cdot \mathbf{n} \rangle_{\partial K}. \end{aligned}$$

Proof. For any $v_h = \{v_0, v_b\} \in \mathcal{V}_h^0$, we test equation (1.1) against v_0 on each element $K \in \mathcal{T}_h$ to obtain

$$\begin{aligned} (f, v_0) &= (u_t, v_0) - \sum_{K \in \mathcal{T}_h} (\nabla \cdot (a \nabla u), v_0)_K \\ &= (\mathcal{Q}_h u_t, v_0) + \sum_{K \in \mathcal{T}_h} (a \nabla u, \nabla v_0)_K - \sum_{K \in \mathcal{T}_h} \langle a \nabla u \cdot \mathbf{n}, v_0 \rangle_{\partial K} \\ &= ((\mathcal{Q}_h u)_t, v_0) + \sum_{K \in \mathcal{T}_h} (a \nabla u, \nabla v_0)_K - \sum_{K \in \mathcal{T}_h} \langle a \nabla u \cdot \mathbf{n}, v_0 - v_b \rangle_{\partial K}, \quad (3.4) \end{aligned}$$

where we have used the divergence theorem and the fact that

$$\sum_{K \in \mathcal{T}_h} \langle a \nabla u \cdot \mathbf{n}, v_b \rangle_{\partial K} = 0.$$

Combining (3.1) and (3.4), we have

$$\begin{aligned}
(u_{ht}, v_0) + \mathcal{A}(u_h, v_h) &= ((\mathcal{Q}_h u)_t, v_0) + \sum_{K \in \mathcal{T}_h} (a \nabla u, \nabla v_0)_K \\
&\quad - \sum_{K \in \mathcal{T}_h} \langle a \nabla u \cdot \mathbf{n}, v_0 - v_b \rangle_{\partial K}.
\end{aligned} \tag{3.5}$$

Then integration by parts together with the identity (2.6) and the definition of \mathbb{Q}_l operator yields

$$\begin{aligned}
&(a \nabla_w \mathcal{Q}_h u, \nabla_w v)_K \\
&= (\nabla_w \mathcal{Q}_h u, \mathbb{Q}_l(a \nabla_w v))_K \\
&= \left(\nabla \mathcal{Q}_k^0 u, \mathbb{Q}_l(a \nabla_w v) \right)_K + \langle \mathcal{Q}_j^b u - \mathcal{Q}_k^0 u, \mathbb{Q}_l(a \nabla_w v) \cdot \mathbf{n} \rangle_{\partial K} \\
&= \left(\mathbb{Q}_l(a \mathbb{Q}_l(\nabla \mathcal{Q}_k^0 u)), \nabla_w v \right)_K + \langle \mathcal{Q}_j^b u - \mathcal{Q}_k^0 u, \mathbb{Q}_l(a \nabla_w v) \cdot \mathbf{n} \rangle_{\partial K} \\
&= \left(\mathbb{Q}_l(a \mathbb{Q}_l(\nabla \mathcal{Q}_k^0 u)), \nabla v_0 \right)_K + \langle \mathcal{Q}_j^b u - \mathcal{Q}_k^0 u, \mathbb{Q}_l(a \nabla_w v) \cdot \mathbf{n} \rangle_{\partial K} \\
&\quad + \langle v_b - v_0, \mathbb{Q}_l(a \mathbb{Q}_l(\nabla \mathcal{Q}_k^0 u)) \cdot \mathbf{n} \rangle_{\partial K},
\end{aligned}$$

so that

$$\begin{aligned}
\mathcal{A}(\mathcal{Q}_h u, v_h) &= \sum_{K \in \mathcal{T}_h} (a \nabla_w \mathcal{Q}_h u, \nabla_w v_h)_K + \mathcal{S}(\mathcal{Q}_h u, v_h) \\
&= \sum_{K \in \mathcal{T}_h} \left(\mathbb{Q}_l(a \mathbb{Q}_l(\nabla \mathcal{Q}_k^0 u)), \nabla v_0 \right)_K + \sum_{K \in \mathcal{T}_h} \langle \mathcal{Q}_j^b u - \mathcal{Q}_k^0 u, \mathbb{Q}_l(a \nabla_w v) \cdot \mathbf{n} \rangle_{\partial K} \\
&\quad + \sum_{K \in \mathcal{T}_h} \langle v_b - v_0, \mathbb{Q}_l(a \mathbb{Q}_l(\nabla \mathcal{Q}_k^0 u)) \cdot \mathbf{n} \rangle_{\partial K} + \mathcal{S}(\mathcal{Q}_h u, v_h),
\end{aligned}$$

and hence,

$$\begin{aligned}
&((\mathcal{Q}_h u)_t, v_0) + \mathcal{A}(\mathcal{Q}_h u, v_h) \\
&= ((\mathcal{Q}_h u)_t, v_0) + \sum_{K \in \mathcal{T}_h} \left(\mathbb{Q}_l(a \mathbb{Q}_l(\nabla \mathcal{Q}_k^0 u)), \nabla v_0 \right)_K \\
&\quad + \sum_{K \in \mathcal{T}_h} \langle \mathcal{Q}_j^b u - \mathcal{Q}_k^0 u, \mathbb{Q}_l(a \nabla_w v) \cdot \mathbf{n} \rangle_{\partial K} \\
&\quad + \sum_{K \in \mathcal{T}_h} \langle v_b - v_0, \mathbb{Q}_l(a \mathbb{Q}_l(\nabla \mathcal{Q}_k^0 u)) \cdot \mathbf{n} \rangle_{\partial K} + \mathcal{S}(\mathcal{Q}_h u, v_h). \tag{3.6}
\end{aligned}$$

Subtracting (3.5) from (3.6) leads to desire result. \square

Next, for a shape regular weak Galerkin discretization \mathcal{T}_h , we recall following crucial estimates for the bilinear maps l_1 , l_2 and l_3 from literature [37].

Lemma 3.2. *Let $\sigma = \min\{l+1, k\}$. Assume that $u \in H^{\sigma+1}(\Omega) \cap H_0^1(\Omega)$ then the following estimate holds true*

$$|l_1(u, v_h)| \leq Ch^\sigma \|u\|_{\sigma+1} \|v_h\|_{1,h} \quad \forall v_h \in \mathcal{V}_h^0,$$

where C is a positive constant depending on $\|a\|_{l+1,\infty}$ -the element wise $W^{l+1,\infty}$ norm of the coefficient matrix a .

Lemma 3.3. *Under the assumptions of Lemma 3.2, for all $v_h \in \mathcal{V}_h^0$, we have*

$$|l_2(u, v_h)| \leq Ch^\sigma \|u\|_{\sigma+1} \|v_h\|_{1,h}.$$

Lemma 3.4. *Let k, j, l be the non-negative integers that define the weak finite element space \mathcal{V}_h . Set $s = \min\{k, j\}$ and assume that $s \geq 1$. In addition, assume that $u \in H^{s+1}(\Omega) \cap H_0^1(\Omega)$ then the following estimate holds true*

$$|l_3(u, v_h)| \leq Ch^s \|u\|_{s+1} \|v_h\|_{1,h} \quad \forall v_h \in \mathcal{V}_h^0.$$

In the case $j \geq l$, we have

$$|l_3(u, v_h)| \leq Ch^k \|u\|_{k+1} \|v_h\|_{1,h} \quad \forall v_h \in \mathcal{V}_h^0. \quad (3.7)$$

3.1 Error estimates with projected element-boundary-discrepancy

Convergence results for the semidiscrete weak Galerkin approximation based on projected element-boundary-discrepancy are presented.

For our convenience, following result is borrowed from [37].

Lemma 3.1.1. *Assume that*

$$\mathcal{S}(u_h, v_h) = \sum_{K \in \mathcal{T}_h} h_K^{-1} \langle \mathcal{Q}_m(u_b - u_0|_{\partial K}), \mathcal{Q}_m(v_b - v_0|_{\partial K}) \rangle_{\partial K},$$

where $\mathcal{Q}_m : L^2(\partial K) \rightarrow \mathcal{P}_m(\partial K)$ is the usual L^2 -projection operator and $m = \max\{j, l\}$. The following results hold true:

(a) *Assume that the solution of (1.1)-(1.2) is so regular that $u \in H^{k+1}(\Omega) \cap H_0^1(\Omega)$ and $j \geq l$, then*

$$|\mathcal{S}(\mathcal{Q}_h u, \mathcal{Q}_h u)| \leq Ch^{2k} \|u\|_{k+1}^2.$$

(b) *Assume that the solution of (1.1)-(1.2) is so regular that $u \in H^{s+1}(\Omega) \cap H_0^1(\Omega)$ and $j < l$, then*

$$|\mathcal{S}(\mathcal{Q}_h u, \mathcal{Q}_h u)| \leq Ch^{2s} \|u\|_{s+1}^2,$$

where $s = \min\{k, j\}$.

The convergence results for the stabilizer with projected element-boundary-discrepancy can be summarized as follows.

Theorem 3.1.1. *Let k, j , and $l \geq k - 1$ be the non-negative integers that define the weak finite element space \mathcal{V}_h . Assume that*

$$\mathcal{S}(u_h, v_h) = \sum_{K \in \mathcal{T}_h} h_K^{-1} \langle \mathcal{Q}_m(u_b - u_0|_{\partial K}), \mathcal{Q}_m(v_b - v_0|_{\partial K}) \rangle_{\partial K},$$

where $\mathcal{Q}_m : L^2(\partial K) \rightarrow \mathcal{P}_m(\partial K)$ is the usual L^2 -projection operator and $m = \max\{j, l\}$. Then the following error estimates hold true:

(a) *For $j < l$, set $s = \min\{k, j\}$ and assume $s \geq 1$. Assume that the solution of (1.1)-(1.2) is so regular that $u \in H^{s+1}(\Omega) \cap H_0^1(\Omega)$. Then*

$$\|e_h(t)\|^2 + \int_0^t \|e_h\|_{1,h}^2 ds \leq C \left(\|e_h(0)\|^2 + h^{2s} \int_0^t \|u\|_{s+1}^2 ds \right), \quad (3.8)$$

$$\begin{aligned} & \int_0^t \|e_{ht}(t)\|^2 ds + \|e_h(t)\|_{1,h}^2 \\ & \leq C \left(\|e_h(0)\|^2 + \|e_{ht}(0)\|^2 + h^{2s} \int_0^t \|u\|_{s+1}^2 ds \right). \end{aligned} \quad (3.9)$$

(b) For $j \geq l$, assume that the solution of (1.1)-(1.2) is so regular that $u \in H^{k+1}(\Omega) \cap H_0^1(\Omega)$. Then

$$\|e_h(t)\|^2 + \int_0^t \|e_h\|_{1,h}^2 ds \leq C \left(\|e_h(0)\|^2 + h^{2k} \int_0^t \|u\|_{k+1}^2 ds \right), \quad (3.10)$$

$$\begin{aligned} & \int_0^t \|e_{ht}(t)\|^2 ds + \|e_h(t)\|_{1,h}^2 \\ & \leq C \left(\|e_h(0)\|^2 + \|e_{ht}(0)\|^2 + h^{2k} \int_0^t \|u\|_{k+1}^2 ds \right). \end{aligned} \quad (3.11)$$

Proof. Set $v_h = e_h$ in the error equation (3.3) to obtain

$$\frac{1}{2} \frac{d}{dt} \|e_h(t)\|^2 + \mathcal{A}(e_h, e_h) \leq |l_1(u, e_h)| + |l_2(u, e_h)| + |l_3(u, e_h)| + |\mathcal{S}(\mathcal{Q}_h u, e_h)|.$$

Then by integrating from 0 to t and using the coercive inequality (2.11), we have

$$\begin{aligned} \frac{1}{2} \|e_h(t)\|^2 + C_1 \int_0^t \|e_h\|_{1,h}^2 ds & \leq \int_0^t |l_1(u, e_h)| ds + \int_0^t |l_2(u, e_h)| ds \\ & \quad + \int_0^t |l_3(u, e_h)| ds + \int_0^t |\mathcal{S}(\mathcal{Q}_h u, e_h)| ds \\ & := I_1 + I_2 + I_3 + I_4. \end{aligned} \quad (3.12)$$

For the terms I_1 and I_2 , we first observe that $\sigma = \min\{l+1, k\} = k$. Then, we apply Lemma 3.2 and Lemma 3.3 to have

$$I_1, I_2 \leq Ch^k \int_0^t \|u\|_{k+1} \|e_h\|_{1,h} ds. \quad (3.13)$$

Assume that $j < l$ and $s = \min\{k, j\}$, so that Lemma 3.4 and Lemma 3.1.1 yields

$$I_3, I_4 \leq Ch^s \int_0^t \|u\|_{s+1} \|e_h\|_{1,h} ds. \quad (3.14)$$

Combining (3.12)-(3.14), we have following $L^\infty(L^2)$ norm and $L^2(\|\cdot\|)$ norm error estimates

$$\|e_h(t)\|^2 + \int_0^t \|e_h\|_{1,h}^2 ds \leq C \left\{ \|e_h(0)\|^2 + h^{2s} \int_0^t \|u\|_{s+1}^2 ds \right\}. \quad (3.15)$$

In the last inequality, we have used the standard Young's inequality.

Next, we differentiate (3.3) with respect to t and then set $v_h = e_{ht}$ in the resulting equation to have

$$\begin{aligned} \frac{1}{2} \frac{d}{dt} \|e_{ht}(t)\|^2 + \mathcal{A}(e_{ht}, e_{ht}) & \leq |l_1(u, e_{ht})| + |l_2(u, e_{ht})| \\ & \quad + |l_3(u, e_{ht})| + |\mathcal{S}(\mathcal{Q}_h u, e_{ht})|. \end{aligned}$$

Arguing as in (3.15), we note that

$$\|e_{ht}(t)\|^2 + \int_0^t \|e_{ht}\|_{1,h}^2 ds \leq C \left(\|e_{ht}(0)\|^2 + h^{2s} \int_0^t \|u\|_{s+1}^2 ds \right). \quad (3.16)$$

Next, we set $v_h = e_{ht}$ in the error equation (3.3) and arguing as in (3.15), we obtain following error estimate

$$\int_0^t \|e_{ht}(s)\|^2 ds + \|e_h(t)\|_{1,h}^2 \leq C \left(\|e_h(0)\|^2 + \|e_{ht}(0)\|^2 + h^{2s} \int_0^t \|u\|_{s+1}^2 ds \right).$$

Here, we have used the estimate (3.16).

Part (b) can be realized in a similar manner. We omit the details. This completes the rest of the proof. \square

Next, we derive an optimal order of estimate for e_h in L^2 norm, the basic idea applied is to use elliptic projection. For $v \in H^2(\Omega) \cap H_0^1(\Omega)$, we define

$$f_v = -\nabla \cdot (a \nabla v) \text{ in } \Omega.$$

Clearly, $f_v \in L^2(\Omega)$. Define $\mathcal{R}_h : H^2(\Omega) \cap H_0^1(\Omega) \rightarrow \mathcal{V}_h^0$ by

$$\mathcal{A}(\mathcal{R}_h v, v_h) = (f_v, v_h) \quad \forall v_h = \{v_0, v_b\} \in \mathcal{V}_h^0, \quad v \in H^2(\Omega) \cap H_0^1(\Omega). \quad (3.17)$$

It is easy to observe from the definition of elliptic projection and equation (3.1) that

$$(u_{ht}, v_h) + \mathcal{A}(u_h - \mathcal{R}_h u, v_h) = (f, v_h) + (\nabla \cdot (a \nabla u), v_h) = (u_t, v_h), \quad (3.18)$$

for all $v_h = \{v_0, v_b\} \in \mathcal{V}_h^0$. Here, we have used equation (1.1).

Remark 3.1.1. *From the identity (3.18), for $u_h(0) = \mathcal{R}_h \psi$, it is easy to see that*

$$\begin{aligned} (e_{ht}(0), v_h) &= (u_{ht}(0) - \mathcal{Q}_h u_t(0), v_h) \\ &= (u_t(0) - \mathcal{Q}_h u_t(0), v_h) \quad \forall v_h = \{v_0, v_b\} \in \mathcal{V}_h^0, \end{aligned}$$

which implies

$$\|e_{ht}(0)\| \leq \|u_t(0) - \mathcal{Q}_h u_t(0)\| \leq Ch^\lambda \|u_t(0)\|_\lambda, \quad 0 \leq \lambda \leq k. \quad (3.19)$$

Here, we have used standard approximation properties for L^2 projection (see, Lemma 4.1 in [39]). Again, from the equation (1.1) it follows that

$$\|u_t(0)\|_\lambda \leq C(\|\psi\|_{\lambda+2} + \|f\|_{H^1(J; H^\lambda)}). \quad (3.20)$$

Combining estimates (3.19) and (3.20), we obtain

$$\|e_{ht}(0)\| \leq Ch^\lambda (\|\psi\|_{\lambda+2} + \|f\|_{H^1(J; H^\lambda)}), \quad 0 \leq \lambda \leq k. \quad (3.21)$$

In view of (3.17), we observe that $\mathcal{R}_h v$ is the WG finite element approximation of the elliptic problem with exact solution $v \in H^2(\Omega) \cap H_0^1(\Omega)$ satisfying following equation

$$-\nabla \cdot (a \nabla v) = f_v \quad \text{in } \Omega. \quad (3.22)$$

Then the error $\rho_v := \mathcal{Q}_h v - \mathcal{R}_h v$ satisfies following error equation (see, Lemma 4.1 in [37])

$$\mathcal{A}(\rho_v, w_h) = l_1(v, w_h) + l_2(v, w_h) + l_3(v, w_h) + \mathcal{S}(\mathcal{Q}_h v, w_h), \quad (3.23)$$

for all $w_h \in \mathcal{V}_h^0$.

Further, following discrete H^1 norm error estimates for R_h hold true [37].

Lemma 3.1.2. *Let k, j , and $l \geq k - 1$ be the non-negative integers that define the weak finite element space \mathcal{V}_h . Assume that*

$$\mathcal{S}(u_h, v_h) = \sum_{K \in \mathcal{T}_h} h_K^{-1} \langle \mathcal{Q}_m(u_b - u_0|_{\partial K}), \mathcal{Q}_m(v_b - v_0|_{\partial K}) \rangle_{\partial K},$$

where $\mathcal{Q}_m : L^2(\partial K) \rightarrow \mathcal{P}_m(\partial K)$ is the usual L^2 projection operator and $m = \max\{j, l\}$. Then the following error estimates hold true:

(a) For $j < l$, set $s = \min\{k, j\}$ and assume $s \geq 1$. For $v \in H^{s+1}(\Omega) \cap H_0^1(\Omega)$, we have

$$\|\mathcal{Q}_h v - \mathcal{R}_h v\|_{1,h} \leq Ch^s \|v\|_{s+1}. \quad (3.24)$$

(b) For $j \geq l$ and $v \in H^{k+1}(\Omega) \cap H_0^1(\Omega)$. Then

$$\|\mathcal{Q}_h v - \mathcal{R}_h v\|_{1,h} \leq Ch^k \|v\|_{k+1}. \quad (3.25)$$

Next, the error $e_h = u_h - \mathcal{Q}_h u$ is expressed in terms of standard ρ and θ as

$$e_h(t) = u_h(t) - \mathcal{Q}_h u(t) = \theta(t) - \rho(t), \quad (3.26)$$

where $\rho := \mathcal{Q}_h u - \mathcal{R}_h u$ and $\theta := u_h - \mathcal{R}_h u$.

For $\theta \in \mathcal{V}_h^0$, we note that (cf. [17])

$$(\theta_t, v_h) + \mathcal{A}(\theta, v_h) = (\rho_t, v_h) \quad \forall v_h \in \mathcal{V}_h^0. \quad (3.27)$$

For $v_h = \theta$ in (3.27), we have

$$(\theta_t, \theta) + \|\theta\|^2 \leq \|\rho_t\| \|\theta\|,$$

which leads to

$$\|\theta\|^2 + \int_0^t \|\theta\|^2 ds \leq \|\theta(0)\|^2 + C \int_0^t \|\rho_t\|^2 ds + C \int_0^t \|\theta\|^2 ds.$$

A simple application of Grownwall's inequality yields

$$\|\theta\|^2 \leq C \left(\|\theta(0)\|^2 + \int_0^t \|\rho_t\|^2 ds \right) = C \int_0^t \|\rho_t\|^2 ds, \quad (3.28)$$

where we have used the fact that $\theta(0) = u_h(0) - \mathcal{R}_h u(0) = 0$.

Remark 3.1.2. *To the best of our knowledge, optimal error estimates in L^2 norm for elliptic problems on general WG finite element space*

$$(\mathcal{P}_k(K), \mathcal{P}_j(\partial K), [\mathcal{P}_l(K)]^2)$$

with arbitrary non-negative integers $\{k, j, l\}$ have not been established earlier. Article [37] is only concerned about the discrete H^1 norm convergence. Therefore, we directly can not use optimal convergence results for the term ρ_t in the L^2 norm.

Next, for the L^2 norm error estimate, we now consider the following auxiliary problem: For every $t \in [0, T]$, find $z(t) \in H_0^1(\Omega) \cap H^2(\Omega)$ such that

$$-\nabla \cdot (a \nabla z(t)) = \rho_t(t). \quad (3.29)$$

Then, we may define $z_h(t) := \{z_0(t), z_b(t)\} \in \mathcal{V}_h^0$ as the solution to following discrete elliptic problem

$$\mathcal{A}(z_h(t), v_h) = (\rho_t(t), v_h) \quad \forall v_h \in V_h^0, \quad t \in [0, T]. \quad (3.30)$$

Clearly, z_h is the weak Galerkin finite element approximation to z and satisfies following estimates (cf. [37])

$$\|z - z_h\|_{1,h} \leq Ch\|z\|_2 \leq Ch\|\rho_t\|. \quad (3.31)$$

Here, we have used the standard a priori estimate for elliptic problem and the WG space $(\mathcal{P}_k(K), \mathcal{P}_j(\partial K), [\mathcal{P}_l(K)]^2)$ with k, j and $l \geq k-1$ are non-negative integers.

Setting $v_h = \rho_t$ in (3.30) and further using identity (3.23), we have

$$\begin{aligned} \|\rho_t\|^2 &= \mathcal{A}(z_h, \rho_t) \\ &= l_1(u_t, z_h) + l_2(u_t, z_h) + l_3(u_t, z_h) + \mathcal{S}(Q_h u_t, z_h). \end{aligned} \quad (3.32)$$

Hence, integrating (3.32) from 0 to T , we arrive at following estimate

$$\begin{aligned} \int_0^T \|\rho_t\|^2 ds &\leq \int_0^T l_1(u_t, z_h) ds + \int_0^T l_2(u_t, z_h) ds \\ &\quad + \int_0^T l_3(u_t, z_h) ds + \int_0^T \mathcal{S}(Q_h u_t, z_h) ds \\ &:= I_1 + I_2 + I_3 + I_4. \end{aligned} \quad (3.33)$$

We now estimate each term separately. For the term I_1 , we use the definition of L^2 projection and the fact that $\nabla z_0 \in [\mathcal{P}_{k-1}(K)]^2 \subseteq [\mathcal{P}_l(K)]^2$ to have

$$\begin{aligned} |l_1(u_t, z_h)| &= \left| \sum_{K \in \mathcal{T}_h} \left(\mathbb{Q}_l(a \mathbb{Q}_l \nabla \mathcal{Q}_k^0 u_t) - a \nabla u_t, \nabla z_0 \right)_K \right| \\ &\leq \sum_{K \in \mathcal{T}_h} \left| \left(a \mathbb{Q}_l \nabla \mathcal{Q}_k^0 u_t - a \nabla u_t, \nabla z_0 \right)_K \right| \\ &\leq \sum_{K \in \mathcal{T}_h} \left| \left(a \mathbb{Q}_l \nabla \mathcal{Q}_k^0 u_t - a \nabla \mathcal{Q}_k^0 u_t, \nabla z_0 \right)_K \right| \\ &\quad + \sum_{K \in \mathcal{T}_h} \left| \left(a \nabla \mathcal{Q}_k^0 u_t - a \nabla u_t, \nabla z_0 \right)_K \right| \\ &:= I_{11} + I_{12}. \end{aligned} \quad (3.34)$$

Now, we use approximation properties for L^2 projections to have

$$\begin{aligned} I_{11} &= \sum_{K \in \mathcal{T}_h} \left| \left(\mathbb{Q}_l \nabla \mathcal{Q}_k^0 u_t - \nabla \mathcal{Q}_k^0 u_t, (a - \bar{a}) \nabla z_0 \right)_K \right| \\ &\leq Ch\|a\|_{1,\infty} \sum_{K \in \mathcal{T}_h} \left| \left(\mathbb{Q}_l \nabla \mathcal{Q}_k^0 u_t - \nabla \mathcal{Q}_k^0 u_t, \nabla z_0 \right)_K \right| \\ &\leq Ch\|a\|_{1,\infty} \sum_{K \in \mathcal{T}_h} Ch^{\lambda_1+1} \|\nabla \mathcal{Q}_k^0 u_t\|_{\lambda_1+1,K} \|\nabla z_0\|_K \\ &\leq Ch^{\lambda_1+2} \|a\|_{1,\infty} \|u_t\|_{\lambda_1+2} \|z_h\|_{1,h}. \end{aligned} \quad (3.35)$$

for some non-negative integer $\lambda_1 \leq l$. Here, \bar{a} is the average of a on each element $K \in \mathcal{T}_h$.

For the term I_{12} , we use the shape regularity assumptions described in [39]. For any $K \in \mathcal{T}_h$, we have a shape regular circumscribed simplex $S(K)$ with diameter $h_{S(K)}$ such that $h_{S(K)} \leq \gamma_* h_K$ with a constant $\gamma_* > 0$ independent of $K \in \mathcal{T}_h$. The shape regularity of $S(K)$ implies that the measure of $S(K)$ is proportional to $h_{S(K)}^2$. Then, we obtain

$$\begin{aligned}
I_{12} &\leq \sum_{K \in \mathcal{T}_h} \|a\|_{L^\infty(K)} \|\nabla \mathcal{Q}_k^0 u_t - \nabla u_t\|_K \|\nabla z_0\|_K \\
&\leq C \sum_{K \in \mathcal{T}_h} \|a\|_{2,K} \|\nabla \mathcal{Q}_k^0 u_t - \nabla u_t\|_K \|\nabla z_0\|_K \\
&\leq C \sum_{K \in \mathcal{T}_h} |K|^{\frac{1}{2}} \|a\|_{W^{2,\infty}(K)} \|\nabla \mathcal{Q}_k^0 u_t - \nabla u_t\|_K \|\nabla z_0\|_K \\
&\leq C \sum_{K \in \mathcal{T}_h} |S(K)|^{\frac{1}{2}} \|a\|_{W^{2,\infty}(K)} \|\nabla \mathcal{Q}_k^0 u_t - \nabla u_t\|_K \|\nabla z_0\|_K \\
&\leq C \sum_{K \in \mathcal{T}_h} h_{S(K)} \|a\|_{W^{2,\infty}(K)} \|\nabla \mathcal{Q}_k^0 u_t - \nabla u_t\|_K \|\nabla z_0\|_K \\
&\leq C \sum_{K \in \mathcal{T}_h} h_K \|a\|_{W^{2,\infty}(K)} \|\nabla \mathcal{Q}_k^0 u_t - \nabla u_t\|_K \|\nabla z_0\|_K \\
&\leq C h \|a\|_{2,\infty} C h^{\lambda_2} \|u_t\|_{\lambda_2+1} \|z_h\|_{1,h} \\
&\leq C h^{\lambda_2+1} \|a\|_{2,\infty} \|u_t\|_{\lambda_2+1} \|\rho_t\|, \tag{3.36}
\end{aligned}$$

for some non-negative integer $\lambda_2 \leq k$. In the above estimate, we have used the embedding $H^2(K) \hookrightarrow L^\infty(K)$ for each $K \in \mathcal{T}_h$ (cf. Theorem 1.4.6 in [5]). Set $\lambda = \min\{\lambda_1 + 1, \lambda_2\}$ and combine above estimates (3.34)-(3.36) to obtain

$$I_1 \leq C \|a\|_{2,\infty} h^{\lambda+1} \int_0^T \|u_t\|_{\lambda+1} \|\rho_t\| ds, \quad 0 \leq \lambda \leq k. \tag{3.37}$$

Then, following the lines of proof for the Lemma 4.3 in [37], we obtain

$$\begin{aligned}
I_2 &\leq C \|a\|_{l+1,\infty} h^\lambda \int_0^T \|u_t\|_{\lambda+1} \|z - z_h\|_{1,h} ds \\
&\leq C \|a\|_{l+1,\infty} h^{\lambda+1} \int_0^T \|u_t\|_{\lambda+1} \|\rho_t\| ds, \quad 0 \leq \lambda \leq k. \tag{3.38}
\end{aligned}$$

In the last inequality, we have used (3.31).

For $j < l$ and $s = \min\{k, j\}$, Lemma 4.4 in [37] yields

$$\begin{aligned}
l_3(u_t, z_h) &\leq C h^s \|u_t\|_{s+1} \left(\sum_{K \in \mathcal{T}_h} \|a \nabla_w z_h\|_K^2 \right)^{\frac{1}{2}} \\
&\leq C h^s \|u_t\|_{s+1} \left(\sum_{K \in \mathcal{T}_h} \|a\|_{L^\infty(K)}^2 \|\nabla_w z_h\|_K^2 \right)^{\frac{1}{2}} \\
&\leq C h^s \|u_t\|_{s+1} C h \|a\|_{2,\infty} \|z_h\|_{1,h} \\
&\leq C h^{s+1} \|a\|_{2,\infty} \|u_t\|_{s+1} \|\rho_t\|. \tag{3.39}
\end{aligned}$$

Similarly, for $j \geq l$, we obtain

$$l_3(u_t, z_h) \leq C h^{k+1} \|a\|_{2,\infty} \|u_t\|_{k+1} \|\rho_t\|. \tag{3.40}$$

Combining estimates (3.39)-(3.40), we have

$$I_3 \leq \begin{cases} Ch^{s+1} \|a\|_{2,\infty} \int_0^T \|u_t\|_{s+1} \|\rho_t\| ds & \text{for } j < l, \\ Ch^{k+1} \|a\|_{2,\infty} \int_0^T \|u_t\|_{k+1} \|\rho_t\| ds, & \text{for } j \geq l. \end{cases} \quad (3.41)$$

Here, $s = \min\{k, j\}$.

Again, for the term I_4 , we apply Lemma 4.5 and Lemma 4.7 in [37] to have

$$\begin{aligned} \mathcal{S}(\mathcal{Q}_h u_t, z_h) &= \mathcal{S}(\mathcal{Q}_h u_t, z_h - \mathcal{Q}_h z) + \mathcal{S}(\mathcal{Q}_h u_t, \mathcal{Q}_h z) \\ &\leq Ch^s \|u_t\|_{s+1} \|z_h - \mathcal{Q}_h z\|_{1,h} \\ &\quad + \sum_{K \in \mathcal{T}_h} h_K^{-1} \langle \mathcal{Q}_m(\mathcal{Q}_k^0 u_t - \mathcal{Q}_j^b u_t), \mathcal{Q}_m(\mathcal{Q}_k^0 z - \mathcal{Q}_j^b z) \rangle_{\partial K} \\ &\leq Ch^{s+1} \|u_t\|_{s+1} \|z\|_2 + Ch^s \|u_t\|_2 Ch \|z\|_2 \\ &\leq Ch^{s+1} \|u_t\|_{s+1} \|\rho_t\|, \end{aligned} \quad (3.42)$$

with $j < l$ and $s = \{k, j\}$. Proceeding similarly, for $j \geq l$, we obtain

$$\mathcal{S}(\mathcal{Q}_h u_t, z_h) \leq Ch^{k+1} \|u_t\|_{k+1} \|\rho_t\|. \quad (3.43)$$

Combining estimates (3.42)-(3.43), we have

$$I_4 \leq \begin{cases} Ch^{s+1} \int_0^T \|u_t\|_{s+1} \|\rho_t\| ds & \text{for } j < l, \\ Ch^{k+1} \int_0^T \|u_t\|_{k+1} \|\rho_t\| ds & \text{for } j \geq l, \end{cases} \quad (3.44)$$

with $s = \min\{k, j\}$.

Substituting estimates for I_i ($1 \leq i \leq 4$) in (3.33), we obtain

$$\|\rho(t)\|^2 \leq \int_0^T \|\rho_t\|^2 ds \leq \begin{cases} Ch^{2(s+1)} \int_0^T \|u_t\|_{s+1}^2 ds & \text{for } j < l, \\ Ch^{2(k+1)} \int_0^T \|u_t\|_{k+1}^2 ds & \text{for } j \geq l. \end{cases} \quad (3.45)$$

Finally, use estimate (3.45) in (3.28) to obtain following $L^\infty(L^2)$ norm error estimate.

Theorem 3.1.2. *Let k, j , and $l \geq k - 1$ be the non-negative integers that define the weak finite element space \mathcal{V}_h . Assume that*

$$\mathcal{S}(u_h, v_h) = \sum_{K \in \mathcal{T}_h} h_K^{-1} \langle \mathcal{Q}_m(u_b - u_0|_{\partial K}), \mathcal{Q}_m(v_b - v_0|_{\partial K}) \rangle_{\partial K},$$

where $\mathcal{Q}_m : L^2(\partial K) \rightarrow \mathcal{P}_m(\partial K)$ is the usual L^2 projection operator and $m = \max\{j, l\}$. Then the following error estimates hold true:

(a) For $j < l$, set $s = \min\{k, j\}$ and assume $s \geq 1$. Assume that the solution of (1.1)-(1.2) is so regular that $u_t \in H^{s+1}(\Omega) \cap H_0^1(\Omega)$. Then

$$\|e_h(t)\|^2 \leq Ch^{2(s+1)} \int_0^t \|u_t\|_{s+1}^2 dt. \quad (3.46)$$

(b) For $j \geq l$, assume that the solution of (1.1)-(1.2) is so regular that $u_t \in H^{k+1}(\Omega) \cap H_0^1(\Omega)$. Then

$$\|e_h(t)\|^2 \leq Ch^{2(k+1)} \int_0^t \|u_t\|_{k+1}^2 dt. \quad (3.47)$$

We assume following convergence results for the semidiscrete weak Galerkin approximation with the stabilizer based on element-boundary-discrepancy.

Theorem 3.1.3. *Let k, j , and $l \geq k - 1$ be the non-negative integers that define the weak finite element space \mathcal{V}_h . Assume that*

$$\mathcal{S}(u_h, v_h) = \sum_{K \in \mathcal{T}_h} h_K^{-1} \langle u_b - u_0|_{\partial K}, v_b - v_0|_{\partial K} \rangle_{\partial K}.$$

Then, we have following error estimates

$$\|e_h(t)\| + h\|e_h(t)\|_{1,h} \leq Ch^{s+1} \left(\int_0^T \|u_t\|_{s+1}^2 dt \right)^{\frac{1}{2}}, \quad (3.48)$$

where $s = \min\{k, j\}$.

4 Discrete time WG Finite Element Method

We now turn our attention to some discrete time weak Galerkin procedures. A discrete-in-time scheme based on backward Euler method for approximating exact solution u is discussed in this section. Optimal pointwise-in-time error estimate in both discrete H^1 and L^2 norms are established.

First we divide the time interval $J = [0, T]$ into M equally spaced subintervals $I_n = (t_{n-1}, t_n]$, $n = 1, 2, \dots, M$ with $t_0 = 0$, and $t_M = T$ and $\tau = t_n - t_{n-1}$, the time step. For a sequence $\{p^n\}_{n=0}^M \subset L^2(\Omega)$, we define

$$\partial_\tau p^n = \frac{p^n - p^{n-1}}{\tau}, \quad n = 1, \dots, M.$$

Also, for a continuous mapping $\phi : [0, T] \rightarrow L^2(\Omega)$, we define $\phi^n = \phi(., t_n)$, $0 \leq n \leq M$.

With the above notation, we now introduce the fully discrete weak Galerkin finite element approximation to the problem (1.1)-(1.2): Let $U_h^0 = \mathcal{R}_h \psi$ and $U_h^n = \{U_0^n, U_b^n\} \in V_h^0$ be the fully discrete solution of u at $t = t_n$ which we shall define through the following scheme

$$(\partial_\tau U_h^n, v_h) + \mathcal{A}(U_h^n, v_h) = (f^n, v_h) \quad \forall v_h \in V_h^0, \quad n = 1, \dots, M. \quad (4.1)$$

For fully discrete error estimates, we now split the errors at $t = t_n$ as follows

$$u^n - U_h^n = u^n - \mathcal{Q}_h u^n + \mathcal{Q}_h u^n - U_h^n.$$

We denote our error as

$$e^n = U_h^n - \mathcal{Q}_h u^n = \{e_0^n, e_b^n\}.$$

4.1 Error estimates with projected element-boundary-discrepancy

Convergence results for the fully discrete weak Galerkin approximation with the stabilizer based on projected element-boundary-discrepancy are presented.

Using ρ and θ , error e^n can be further separated as

$$e^n = \theta^n + \rho^n, \quad (4.2)$$

where $\theta^n = U_h^n - \mathcal{R}_h u^n$ and $\rho^n = \mathcal{R}_h u^n - \mathcal{Q}_h u^n$.

For θ^n , we have the following error equation

$$\begin{aligned} (\partial_\tau \theta^n, v_0) + \mathcal{A}(\theta^n, v) &= -(\partial_\tau \mathcal{R}_h u^n - u_t^n, v_0) \\ &:= -(w^n, v_0) \quad \forall v = \{v_0, v_b\} \in V_h^0, \end{aligned} \quad (4.3)$$

where $w^n = \partial_\tau \mathcal{R}_h u^n - u_t^n$. For simplicity of the exposition, we write $w^n = \mathcal{R}_1^n + \mathcal{R}_2^n$, where $\mathcal{R}_1^n = \partial_\tau \mathcal{R}_h u^n - \partial_\tau u^n$ and $\mathcal{R}_2^n = \partial_\tau u^n - u_t^n$.

Set $v = \theta^n$ in (4.3), we have

$$(\partial_\tau \theta^n, \theta^n) + \mathcal{A}(\theta^n, \theta^n) \leq \|w^n\| \|\theta^n\|.$$

Then using the positivity of $\mathcal{A}(\cdot, \cdot)$, we obtain

$$\|\theta^n\| \leq \|\theta^{n-1}\| + \tau \|w^n\|,$$

where we have used the fact that $\theta^0 = U_h^0 - \mathcal{R}_h u^0 = 0$. Hence, we have

$$\|\theta^n\| \leq \tau \sum_{j=1}^n \|w^j\| \leq \tau \sum_{j=1}^n \|\mathcal{R}_1^j\| + \tau \sum_{j=1}^n \|\mathcal{R}_2^j\|. \quad (4.4)$$

For the term \mathcal{R}_1^j , it is easy to verify that

$$\tau \mathcal{R}_1^j = \int_{t_{j-1}}^{t_j} (\mathcal{R}_h u_t - u_t) ds,$$

which together with estimates (3.45) leads to the following

$$\tau \sum_{j=1}^n \|\mathcal{R}_1^j\| \leq \begin{cases} Ch^{(s+1)} \left(\int_0^T \|u_t\|_{s+1}^2 ds \right)^{\frac{1}{2}} & \text{for } j < l, \\ Ch^{k+1} \left(\int_0^T \|u_t\|_{k+1}^2 ds \right)^{\frac{1}{2}} & \text{for } j \geq l. \end{cases} \quad (4.5)$$

Now, for the term \mathcal{R}_2 , we use Taylor's series expansion to have

$$\tau \sum_{j=1}^n \|\mathcal{R}_2^j\| \leq C \tau \int_0^T \|u_{tt}\| ds. \quad (4.6)$$

Finally, estimates (4.4)-(4.6) together with (3.45) leads to following L^2 norm error estimates.

Theorem 4.1.1. *Let k, j and $l \geq k - 1$ be the non-negative integers that define the weak finite element space \mathcal{V}_h . Assume that*

$$\mathcal{S}(u_h, v_h) = \sum_{K \in \mathcal{T}_h} h_K^{-1} \langle \mathcal{Q}_m(u_b - u_0|_{\partial K}), \mathcal{Q}_m(v_b - v_0|_{\partial K}) \rangle_{\partial K},$$

where $\mathcal{Q}_m : L^2(\partial K) \rightarrow \mathcal{P}_m(\partial K)$ is the usual L^2 projection operator and $m = \max\{j, l\}$. Then the following error estimates hold true:

(a) For $j < l$, set $s = \min\{k, j\}$ and assume $s \geq 1$. Assume that the solution of (1.1)-(1.2) is so regular that $u_t \in H^{s+1}(\Omega) \cap H_0^1(\Omega)$. Then

$$\|e^n\|^2 \leq C \left(h^{2(s+1)} + \tau^2 \right) \int_0^T \left(\|u_t\|_{s+1}^2 + \|u_{tt}\|^2 \right) dt. \quad (4.7)$$

(b) For $j \geq l$, assume that the solution of (1.1)-(1.2) is so regular that $u_t \in H^{k+1}(\Omega) \cap H_0^1(\Omega)$. Then

$$\|e^n\|^2 \leq C \left(h^{2(k+1)} + \tau^2 \right) \int_0^T \left(\|u_t\|_{k+1}^2 + \|u_{tt}\|^2 \right) dt. \quad (4.8)$$

Next, setting $v_h = -\tau \partial_\tau \theta^n$ in (4.3), we have

$$\tau \|\partial_\tau \theta^n\|^2 + \mathcal{A}(\theta^n, \theta^n - \theta^{n-1}) \leq \tau \|w^n\| \|\partial_\tau \theta^n\|, \quad (4.9)$$

which yields

$$\begin{aligned} \tau \|\partial_\tau \theta^n\|^2 + \|\theta^n\|^2 - \|\theta^{n-1}\|^2 &\leq C \tau \|w^n\|^2 \\ &\leq C \tau (\|\mathcal{R}_1^n\|^2 + \|\mathcal{R}_2^n\|^2). \end{aligned} \quad (4.10)$$

From (4.5), we note that

$$\tau \mathcal{R}_1^j \leq \tau^{\frac{1}{2}} \left(\int_{t_{j-1}}^{t_j} (\mathcal{R}_h u_t - u_t)^2 dt \right)^{\frac{1}{2}}$$

so that following estimates hold true

$$\tau \sum_{j=1}^n \|\mathcal{R}_1^j\|^2 \leq \begin{cases} Ch^{2(s+1)} \int_0^T \|u_t\|_{s+1}^2 ds & \text{for } j < l, \\ Ch^{2(k+1)} \int_0^T \|u_t\|_{k+1}^2 ds & \text{for } j \geq l. \end{cases} \quad (4.11)$$

Again, we know that

$$\mathcal{R}_2^j = \frac{u^j - u^{j-1}}{\tau} - u_t^j = -\frac{1}{\tau} \int_{t_{j-1}}^{t_j} (s - t_{j-1}) u_{tt} ds.$$

Hence, we have

$$\begin{aligned} |\mathcal{R}_2^j|^2 &\leq \frac{1}{\tau^2} \left(\int_{t_{j-1}}^{t_j} (s - t_{j-1})^2 ds \right) \left(\int_{t_{j-1}}^{t_j} u_{tt}^2 ds \right) \\ &\leq C \tau \int_{t_{j-1}}^{t_j} u_{tt}^2 ds, \end{aligned}$$

which integration over Ω yields

$$\|\mathcal{R}_2^j\|^2 \leq C \tau \int_{t_{j-1}}^{t_j} \|u_{tt}\|^2 ds. \quad (4.12)$$

Now, estimates (4.10)-(4.12) together with (3.45) leads to following discrete H^1 norm error estimates.

Theorem 4.1.2. Let k, j and $l \geq k-1$ be the non-negative integers that define the weak finite element space \mathcal{V}_h . Assume that

$$\mathcal{S}(u_h, v_h) = \sum_{K \in \mathcal{T}_h} h_K^{-1} \langle \mathcal{Q}_m(u_b - u_0|_{\partial K}), \mathcal{Q}_m(v_b - v_0|_{\partial K}) \rangle_{\partial K},$$

where $\mathcal{Q}_m : L^2(\partial K) \rightarrow \mathcal{P}_m(\partial K)$ is the usual L^2 projection operator and $m = \max\{j, l\}$. Then the following error estimates hold true:

(a) For $j < l$, set $s = \min\{k, j\}$ and assume $s \geq 1$. Assume that the solution of (1.1)-(1.2) is so regular that $u_t \in H^{s+1}(\Omega) \cap H_0^1(\Omega)$. Then

$$\|e^n\|^2 \leq C(h^{2s} + \tau^2) \int_0^T (\|u_t\|_{s+1}^2 + \|u_{tt}\|^2) dt. \quad (4.13)$$

(b) For $j \geq l$, assume that the solution of (1.1)-(1.2) is so regular that $u_t \in H^{k+1}(\Omega) \cap H_0^1(\Omega)$. Then

$$\|e^n\|^2 \leq C(h^{2k} + \tau^2) \int_0^T (\|u_t\|_{k+1}^2 + \|u_{tt}\|^2) dt. \quad (4.14)$$

We assume following convergence results for the fully discrete weak Galerkin approximation with the stabilizer based on element-boundary-discrepancy.

Theorem 4.1.3. Let k, j , and $l \geq k - 1$ be the non-negative integers that define the weak finite element space \mathcal{V}_h . Assume that

$$\mathcal{S}(u_h, v_h) = \sum_{K \in \mathcal{T}_h} h_K^{-1} \langle u_b - u_0|_{\partial K}, v_b - v_0|_{\partial K} \rangle_{\partial K}.$$

Then, we have following error estimates

$$\|e^n\|^2 \leq C(h^{2(s+1)} + \tau^2) \int_0^T (\|u_t\|_{s+1}^2 + \|u_{tt}\|^2) dt, \quad (4.15)$$

$$\|e^n\|^2 \leq C(h^{2s} + \tau^2) \int_0^T (\|u_t\|_{s+1}^2 + \|u_{tt}\|^2) dt, \quad (4.16)$$

where $s = \min\{k, j\}$.

Remark 4.1.1. From Theorems 4.1.1-4.1.3 it is clear that the method of projected element-boundary-discrepancy is more accurate than the method of element-boundary-discrepancy for the case of $j = k - 1$ and $l = k - 1$. For the numerical validation, we refer to Tables 1-8.

5 Numerical Experiments

In this section we will explore the results of computations for the parabolic problems (1.1)-(1.2) in $\Omega \times J$, where $\Omega = (0, 1) \times (0, 1)$ and $J = [0, 1]$ with selected values on the degree of polynomials in the weak Galerkin finite element space. The coefficient matrix a is given by identity matrix I , the load function f , initial data ψ and the Dirichlet boundary value are selected in such a way that exact solution is $u = \exp(-t) \sin(\pi x) \sin(\pi y)$. In this test problem, triangular mesh is used. We have done uniform partitioning of the domain into $n \times n$ sub rectangles which is followed by dividing each rectangular element by the diagonal line with mesh size $h = 1/n$, where n is any non-negative integer. Further, we set $\tau = O(h^{\gamma+1})$, where γ is selected according to Theorems 4.1.1-4.1.3 so that optimal order of convergence is maintained.

Let U_h^n be the weak Galerkin solution defined by (4.1). Then, we have calculated the following error

$$e^n = U_h^n - \mathcal{Q}_h u^n = \{e_0^n, e_b^n\},$$

with respect to triple bar norm and the L^2 norm at final time $T = 1$.

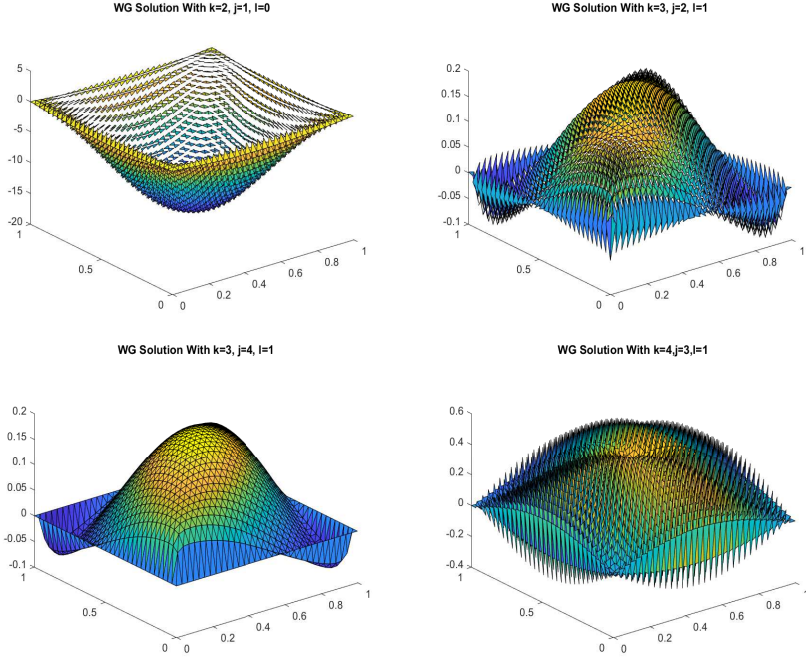


Figure 1: Plots of the WG approximations at time $t = 1$ for the method of projected element-boundary-discrepancy with $h = 1/32$.

Recall that the stabilizer for the method of projected element-boundary-discrepancy is given by

$$\mathcal{S}(u_h, v_h) = \sum_{K \in \mathcal{T}_h} h_K^{-1} \langle \mathcal{Q}_m(u_b - u_0|_{\partial K}), \mathcal{Q}_m(v_b - v_0|_{\partial K}) \rangle_{\partial K},$$

where $m = \min\{j, l\}$. For different values of k ($1 \leq k \leq 4$), j ($0 \leq j \leq 4$) and l ($0 \leq l \leq 4$), we have implemented the corresponding WG scheme (4.1) for the problem (1.1)-(1.2). The rate of convergence for each combination is reported in Tables 1-4, where NI means the corresponding WG scheme is unstable or not consistent. Detailed computational data can be found in the Appendix. The convergence order for each particular combination is indicated in the form n/m , where n stand for the order of convergence in the triple bar norm and m for the order of convergence in the L^2 norm. For example, $2/3$ would mean that the method is convergent at the rate of h^2 in the triple bar norm and h^3 in the L^2 norm. For $l < k - 1$, the method works poorly. This is an observation from the computation. For instance, we refer to Figure 1.

The method of element-boundary-discrepancy is based on the selection of stabilizer $\mathcal{S}(u_h, v_h) = \sum_{K \in \mathcal{T}_h} h_K^{-1} \langle u_b - u_0|_{\partial K}, v_b - v_0|_{\partial K} \rangle_{\partial K}$. For all the values of $k = 1, \dots, 4$, $j = 0, \dots, 4$, and $l = 0, \dots, 4$, we have implemented the corresponding WG finite element scheme (4.1). The order of convergence for each combination is listed in Tables 5-8. Tables 5-8 suggest that the WG algorithms corresponding to the case of $l = k - 2$ and $j < k$ are solvable. For $l = k - 2$ with $j \geq k$ and $l < k - 2$, the method is solvable but not consistent. At present, we do

not have mathematical justification. This is an observation from the numerical experiments, which is illustrated in Figure 2.

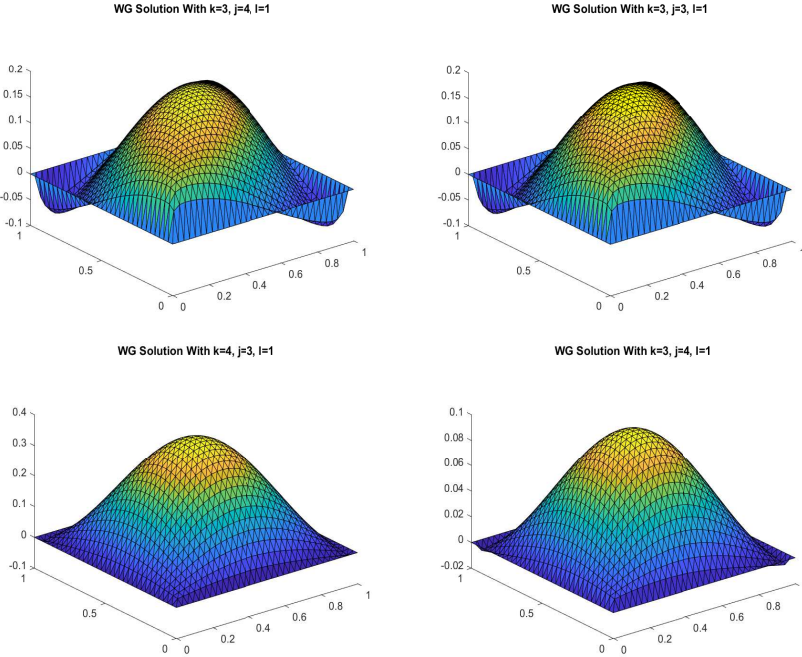


Figure 2: Plots of the WG approximations at time $t = 1$ for the method of element-boundary-discrepancy with $h = 1/32$.

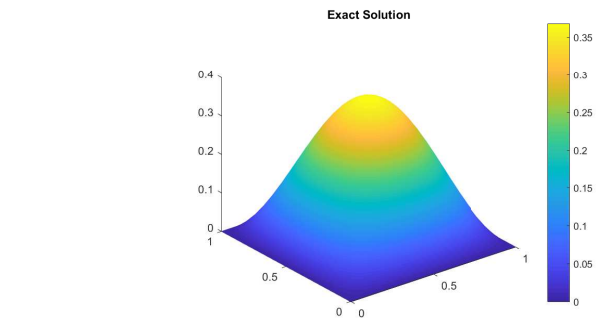


Figure 3: Exact solution at $t = 1$.

6 Concluding Remarks

In this paper we have conducted a systematic study for the WG-FEM with local elements ($\mathcal{P}_k(K)$, $\mathcal{P}_j(\partial K)$, $[\mathcal{P}_l(K)]^2$). For all values of k , j and l , we have

established a theoretical framework for the convergence and error estimates in the triple bar norm and standard L^2 norm. The results are summarized as follows.

- (A) For the method of projected element-boundary-discrepancy, we have the following results:
 - (i) For $l \geq k - 1$ and $j \geq l$, the corresponding WG scheme is stable and the convergence order of k in the triple bar norm and $k + 1$ in L^2 norm.
 - (ii) For $l \geq k - 1$ and $j < l$, the corresponding WG scheme is stable and has convergence order of $s = \min\{k, j\}$ in the triple bar norm and $s + 1$ in L^2 norm.
 - (iii) For $l < k - 1$, the corresponding WG scheme is either unstable or not consistent.
- (B) For the stabilizer with element-boundary-discrepancy, the following results hold true:
 - (i) For $l \geq k - 1$, the corresponding WG scheme is stable and the convergence order of $s = \min\{k, j\}$ in the triple bar norm and $s + 1$ in L^2 norm.
 - (ii) For $l = k - 2$ and $j < k$, the corresponding WG scheme is stable and the convergence order of $s = \min\{k, j\}$ in the triple bar norm.
 - (iii) For $l = k - 2$ with $j \geq k$ and $l < k - 2$ the corresponding WG scheme is solvable but not consistent.

Numerical results are presented for triangular meshes. It would be very challenging to develop weak Galerkin solver for parabolic equation with weak Galerkin space $(\mathcal{P}_k(K), \mathcal{P}_j(\partial K), [\mathcal{P}_l(K)]^2)$, where $k \geq 1$, $j \geq 0$ and $l \geq 0$ are arbitrary integers, for polygonal meshes. Currently, we are working on it for second order Crank-Nicolson scheme. For the possible extension of this work, we refer to second-order parabolic partial differential equations with non-classic boundary conditions (cf. [1, 12, 13, 14, 15, 16]).

References

- [1] M. Abbaszadeh and M. Dehghan. Meshless local numerical procedure based on interpolating moving least squares approximation and exponential time differencing fourth-order runge–kutta (etdrk4) for solving stochastic parabolic interface problems. *Engineering with Computers*, pages 1–21, 2020.
- [2] R. Adams and J. Fournier. *Sobolev Spaces, sec. ed.* Academic Press, Amsterdam, 2003.
- [3] D. N. Arnold, F. Brezzi, B. Cockburn, and L. D. Marini. Unified analysis of discontinuous galerkin methods for elliptic problems. *SIAM journal on numerical analysis*, 39(5):1749–1779, 2002.
- [4] L. Beirão da Veiga, F. Brezzi, A. Cangiani, G. Manzini, L. D. Marini, and A. Russo. Basic principles of virtual element methods. *Mathematical Models and Methods in Applied Sciences*, 23(01):199–214, 2013.

- [5] S. Brenner and R. Scott. *The mathematical theory of finite element methods*, volume 15. Springer Science & Business Media, 2007.
- [6] A. Cangiani, Z. Dong, and E. H. Georgoulis. hp-version space-time discontinuous galerkin methods for parabolic problems on prismatic meshes. *SIAM Journal on Scientific Computing*, 39(4):A1251–A1279, 2017.
- [7] A. Cangiani, E. H. Georgoulis, and P. Houston. hp-version discontinuous Galerkin methods on polygonal and polyhedral meshes. *Mathematical Models and Methods in Applied Sciences*, 24(10):2009–2041, 2014.
- [8] B. Cockburn. The weak galerkin methods are rewritings of the hybridizable discontinuous galerkin methods. *arXiv preprint arXiv:1812.08146*, 2018.
- [9] B. Cockburn, D. A. Di Pietro, and A. Ern. Bridging the hybrid high-order and hybridizable discontinuous galerkin methods. *ESAIM: Mathematical Modelling and Numerical Analysis*, 50(3):635–650, 2016.
- [10] B. Cockburn, J. Gopalakrishnan, and R. Lazarov. Unified hybridization of discontinuous galerkin, mixed, and continuous galerkin methods for second order elliptic problems. *SIAM Journal on Numerical Analysis*, 47(2):1319–1365, 2009.
- [11] L. B. da Veiga and G. Manzini. A virtual element method with arbitrary regularity. *IMA Journal of Numerical Analysis*, 34(2):759–781, 2014.
- [12] M. Dehghan. A new adi technique for two-dimensional parabolic equation with an integral condition. *Computers & Mathematics with Applications*, 43(12):1477–1488, 2002.
- [13] M. Dehghan. Efficient techniques for the second-order parabolic equation subject to nonlocal specifications. *Applied Numerical Mathematics*, 52(1):39–62, 2005.
- [14] M. Dehghan. A computational study of the one-dimensional parabolic equation subject to nonclassical boundary specifications. *Numerical Methods for Partial Differential Equations*, 22(1):220–257, 2006.
- [15] M. Dehghan. The one-dimensional heat equation subject to a boundary integral specification. *Chaos, Solitons & Fractals*, 32(2):661–675, 2007.
- [16] M. Dehghan and M. Shamsi. Numerical solution of two-dimensional parabolic equation subject to nonstandard boundary specifications using the pseudospectral legendre method. *Numerical Methods for Partial Differential Equations*, 22(6):1255–1266, 2006.
- [17] B. Deka and P. Roy. Weak Galerkin finite element methods for parabolic interface problems with nonhomogeneous jump conditions. *Numerical Functional Analysis and Optimization*, 40(3):259–279, 2019.
- [18] H. Li, L. Mu, and X. Ye. Interior energy error estimates for the weak Galerkin finite element method. *Numerische Mathematik*, 139(2):447–478, 2018.
- [19] Q. H. Li and J. Wang. Weak Galerkin finite element methods for parabolic equations. *Numerical Methods for Partial Differential Equations*, 29(6):2004–2024, 2013.

- [20] R. Lin, X. Ye, S. Zhang, and P. Zhu. A weak Galerkin finite element method for singularly perturbed convection-diffusion-reaction problems. *SIAM Journal on Numerical Analysis*, 56(3):1482–1497, 2018.
- [21] J. Liu, S. Tavener, and Z. Wang. Lowest-order weak Galerkin finite element method for darcy flow on convex polygonal meshes. *SIAM Journal on Scientific Computing*, 40(5):B1229–B1252, 2018.
- [22] J. Liu, S. Tavener, and Z. Wang. Penalty-free any-order weak galerkin fems for elliptic problems on quadrilateral meshes. *Journal of Scientific Computing*, 83:47, 2020.
- [23] X. Liu, J. Li, and Z. Chen. A weak Galerkin finite element method for the oseen equations. *Advances in Computational Mathematics*, 42(6):1473–1490, 2016.
- [24] J. Mélek, J. Nečas, M. Rokyta, and M. Ružička. *Weak and measure-valued solutions to evolutionary PDEs*, volume 13. Chapman & Hall, London, UK, 1996.
- [25] L. Mu. Pressure robust weak galerkin finite element methods for stokes problems. *SIAM Journal on Scientific Computing*, 42(3):B608–B629, 2020.
- [26] L. Mu. A uniformly robust h (div) weak galerkin finite element methods for brinkman problems. *SIAM Journal on Numerical Analysis*, 58(3):1422–1439, 2020.
- [27] L. Mu, J. Wang, and X. Ye. A least-squares-based weak Galerkin finite element method for second order elliptic equations. *SIAM Journal on Scientific Computing*, 39(4):A1531–A1557, 2017.
- [28] L. Mu, J. Wang, and X. Ye. A weak Galerkin method for the reissner-mindlin plate in primary form. *Journal of Scientific Computing*, 75(2):782–802, 2018.
- [29] L. Mu, J. Wang, X. Ye, and S. Zhang. A weak Galerkin finite element method for the maxwell equations. *Journal of Scientific Computing*, 65(1):363–386, 2015.
- [30] L. Mu, J. Wang, X. Ye, and S. Zhao. A new weak Galerkin finite element method for elliptic interface problems. *Journal of Computational Physics*, 325:157–173, 2016.
- [31] S. Shields, J. Li, and E. A. Machorro. Weak Galerkin methods for time-dependent maxwell’s equations. *Computers & Mathematics with Applications*, 74(9):2106–2124, 2017.
- [32] L. Song, S. Zhao, and K. Liu. A relaxed weak Galerkin method for elliptic interface problems with low regularity. *Applied Numerical Mathematics*, 128:65–80, 2018.
- [33] V. Thomée. *Galerkin finite element methods for parabolic problems*, volume 1054. Springer, 1984.
- [34] G. Vacca and L. Beirão da Veiga. Virtual element methods for parabolic problems on polygonal meshes. *Numerical Methods for Partial Differential Equations*, 31(6):2110–2134, 2015.

- [35] C. Wang and J. Wang. Discretization of div–curl systems by weak Galerkin finite element methods on polyhedral partitions. *Journal of Scientific Computing*, 68(3):1144–1171, 2016.
- [36] C. Wang and J. Wang. A primal-dual weak Galerkin finite element method for second order elliptic equations in non-divergence form. *Mathematics of Computation*, 87(310):515–545, 2018.
- [37] J. Wang, R. Wang, Q. Zhai, and R. Zhang. A systematic study on weak Galerkin finite element methods for second order elliptic problems. *Journal of Scientific Computing*, 74(3):1369–1396, 2018.
- [38] J. Wang and X. Ye. A weak Galerkin finite element method for second-order elliptic problems. *Journal of Computational and Applied Mathematics*, 241:103–115, 2013.
- [39] J. Wang and X. Ye. A weak Galerkin mixed finite element method for second order elliptic problems. *Mathematics of Computation*, 83(289):2101–2126, 2014.
- [40] J. Wang and X. Ye. A weak Galerkin finite element method for the stokes equations. *Advances in Computational Mathematics*, 42(1):155–174, 2016.
- [41] J. Wang and X. Ye. The basics of weak galerkin finite element methods. *arXiv preprint arXiv:1901.10035*, 2019.
- [42] S. Xie, P. Zhu, and X. Wang. Error analysis of weak Galerkin finite element methods for time-dependent convection–diffusion equations. *Applied Numerical Mathematics*, 137:19–33, 2019.
- [43] H. Zhang, Y. Zou, Y. Xu, Q. Zhai, and H. Yue. Weak Galerkin finite element method for second order parabolic equations. *Int. J. Numer. Anal. Model.*, 13(4):525–544, 2016.
- [44] L. Zhang, M. Feng, and J. Zhang. A globally divergence-free weak Galerkin method for brinkman equations. *Applied Numerical Mathematics*, 137:213–229, 2019.
- [45] S. Zhou, F. Gao, B. Li, and Z. Sun. Weak Galerkin finite element method with second-order accuracy in time for parabolic problems. *Applied Mathematics Letters*, 90:118–123, 2019.

Appendix

In this section we demonstrate some detailed numerical results for a set of selected values of k, j and l . These results will be in support of the rate of convergence reported in Section 5. The numerical results are organized as follows. Tables 9-14 illustrate the table index numbers for the set value of (k, j, l) , and the rest of the tables show the corresponding numerical results. For example, Table 9 points to the table index numbers when the stabilizer $\mathcal{S}(u_h, v_h) = \sum_{K \in \mathcal{T}_h} h_K^{-1} \langle \mathcal{Q}_m(u_h - u_0|_{\partial K}), \mathcal{Q}_m(v_h - v_0|_{\partial K}) \rangle_{\partial K}$ was employed in the numerical scheme. This table has a fixed value of $k = 2$ while j and l are varying. The entry of the table at $(k, j, l) = (2, 1, 2)$ has value Table 17, so that the computational results for $(k, j, l) = (2, 1, 2)$ should be found in Table 17.

Index Tables

The index tables are given in Tables 9, 10, 11, 12, 13, and 14. Here, note that the values in those tables refer to the table number where the computational results are reported.

Tables for Computational Results

All the detailed numerical results are provided in Tables 15-43. No interpretation of the data is necessary as they are virtually self-explanatory. Interested readers are invited to draw their own conclusions from reading these numerical results.

Table 1: Order of convergence for $k=1$ with stabilizer term $h_K^{-1}\langle \mathcal{Q}_m(u_b - u_0|_{\partial K}), \mathcal{Q}_m(v_b - v_0|_{\partial K}) \rangle$

$k = 1$	$j = 0$	$j = 1$	$j = 2$	$j = 3$	$j = 4$
$l = 0$	1/2	1/2	1/2	1/2	1/2
$l = 1$	0/0	1/2	1/2	1/2	1/2
$l = 2$	0/0	1/2	1/2	1/2	1/2
$l = 3$	0/0	1/2	1/2	1/2	1/2
$l = 4$	0/0	1/2	1/2	1/2	1/2

Table 2: Order of convergence for $k=2$ with stabilizer term $h_K^{-1}\langle \mathcal{Q}_m(u_b - u_0|_{\partial K}), \mathcal{Q}_m(v_b - v_0|_{\partial K}) \rangle$

$k = 2$	$j = 0$	$j = 1$	$j = 2$	$j = 3$	$j = 4$
$l = 0$	NI	NI	NI	NI	NI
$l = 1$	0/0	2/3	2/3	2/3	2/3
$l = 2$	0/0	1/2	2/3	2/3	2/3
$l = 3$	0/0	1/2	2/3	2/3	2/3
$l = 4$	0/0	1/2	2/3	2/3	2/3

Table 3: Order of convergence for $k=3$ with stabilizer term $h_K^{-1}\langle \mathcal{Q}_m(u_b - u_0|_{\partial K}), \mathcal{Q}_m(v_b - v_0|_{\partial K}) \rangle$

$k = 3$	$j = 0$	$j = 1$	$j = 2$	$j = 3$	$j = 4$
$l = 0$	NI	NI	NI	NI	NI
$l = 1$	NI	NI	NI	NI	NI
$l = 2$	0/0	1/2	3/4	3/4	3/4
$l = 3$	0/0	1/2	2/3	3/4	3/4
$l = 4$	0/0	1/2	2/3	3/4	3/4

Table 4: Order of convergence for $k=4$ with stabilizer term $h_K^{-1}\langle \mathcal{Q}_m(u_b - u_0|_{\partial K}), \mathcal{Q}_m(v_b - v_0|_{\partial K}) \rangle$

$k = 4$	$j = 0$	$j = 1$	$j = 2$	$j = 3$	$j = 4$
$l = 0$	NI	NI	NI	NI	NI
$l = 1$	NI	NI	NI	NI	NI
$l = 2$	NI	NI	NI	NI	NI
$l = 3$	0/0	1/2	2/3	4/5	4/5
$l = 4$	0/0	1/2	2/3	3/4	4/5

Table 5: Order of convergence for $k=1$ with stabilizer term $h_K^{-1}\langle u_b - u_0|_{\partial K}, v_b - v_0|_{\partial K} \rangle$

$k = 1$	$j = 0$	$j = 1$	$j = 2$	$j = 3$	$j = 4$
$l = 0$	0/0	1/2	1/2	1/2	1/2
$l = 1$	0/0	1/2	1/2	1/2	1/2
$l = 2$	0/0	1/2	1/2	1/2	1/2
$l = 3$	0/0	1/2	1/2	1/2	1/2
$l = 4$	0/0	1/2	1/2	1/2	1/2

Table 6: Order of convergence for $k=2$ with stabilizer term
 $h_K^{-1}\langle u_b - u_0|_{\partial K}, v_b - v_0|_{\partial K} \rangle$

$k = 2$	$j = 0$	$j = 1$	$j = 2$	$j = 3$	$j = 4$
$l = 0$	0/0	1/2	NI	NI	NI
$l = 1$	0/0	1/2	2/3	2/3	2/3
$l = 2$	0/0	1/2	2/3	2/3	2/3
$l = 3$	0/0	1/2	2/3	2/3	2/3
$l = 4$	0/0	1/2	2/3	2/3	2/3

Table 7: Order of convergence for $k=3$ with stabilizer term
 $h_K^{-1}\langle u_b - u_0|_{\partial K}, v_b - v_0|_{\partial K} \rangle$

$k = 3$	$j = 0$	$j = 1$	$j = 2$	$j = 3$	$j = 4$
$l = 0$	NI	NI	NI	NI	NI
$l = 1$	0/0	1/2	2/3	NI	NI
$l = 2$	0/0	1/2	2/3	3/4	3/4
$l = 3$	0/0	1/2	2/3	3/4	3/4
$l = 4$	0/0	1/2	2/3	3/4	3/4

Table 8: Order of convergence for $k=4$ with stabilizer term
 $h_K^{-1}\langle u_b - u_0|_{\partial K}, v_b - v_0|_{\partial K} \rangle$

$k = 4$	$j = 0$	$j = 1$	$j = 2$	$j = 3$	$j = 4$
$l = 0$	NI	NI	NI	NI	NI
$l = 1$	NI	NI	NI	NI	NI
$l = 2$	0/0	1/2	2/3	3/4	NI
$l = 3$	0/0	1/2	2/3	3/4	4/5
$l = 4$	0/0	1/2	2/3	3/4	4/5

Table 9: Order of convergence for $k=2$ with stabilizer term
 $h_K^{-1}\langle \mathcal{Q}_m(u_b - u_0|_{\partial K}), \mathcal{Q}_m(v_b - v_0|_{\partial K}) \rangle$

$k = 2$	$j = 0$	$j = 1$	$j = 2$	$j = 3$	$j = 4$
$l = 0$					
$l = 1$	Table 15	Table 16			
$l = 2$		Table 17	Table 18		
$l = 3$				Table 19	
$l = 4$					Table 20

Table 10: Order of convergence for $k=3$ with stabilizer term
 $h_K^{-1}\langle \mathcal{Q}_m(u_b - u_0|_{\partial K}), \mathcal{Q}_m(v_b - v_0|_{\partial K}) \rangle$

$k = 3$	$j = 0$	$j = 1$	$j = 2$	$j = 3$	$j = 4$
$l = 0$					
$l = 1$					
$l = 2$		Table 21	Table 22		
$l = 3$			Table 23	Table 24	
$l = 4$					Table 25

Table 11: Order of convergence for $k=4$ with stabilizer term

$$h_K^{-1} \langle \mathcal{Q}_m(u_b - u_0|_{\partial K}, v_b - v_0|_{\partial K}) \rangle$$

$k = 4$	$j = 0$	$j = 1$	$j = 2$	$j = 3$	$j = 4$
$l = 0$					
$l = 1$					
$l = 2$					
$l = 3$		Table 26	Table 27	Table 28	
$l = 4$				Table 29	Table 30

Table 12: Order of convergence for $k=2$ with stabilizer term

$$h_K^{-1} \langle u_b - u_0|_{\partial K}, v_b - v_0|_{\partial K} \rangle$$

$k = 2$	$j = 0$	$j = 1$	$j = 2$	$j = 3$	$j = 4$
$l = 0$					
$l = 1$		Table 31			
$l = 2$			Table 32		
$l = 3$				Table 33	
$l = 4$					Table 34

Table 13: Order of convergence for $k=3$ with stabilizer term

$$h_K^{-1} \langle u_b - u_0|_{\partial K}, v_b - v_0|_{\partial K} \rangle$$

$k = 3$	$j = 0$	$j = 1$	$j = 2$	$j = 3$	$j = 4$
$l = 0$					
$l = 1$		Table 35			
$l = 2$			Table 36		
$l = 3$				Table 37	
$l = 4$					Table 38

Table 14: Order of convergence for $k=4$ with stabilizer term

$$h_K^{-1} \langle u_b - u_0|_{\partial K}, v_b - v_0|_{\partial K} \rangle$$

$k = 4$	$j = 0$	$j = 1$	$j = 2$	$j = 3$	$j = 4$
$l = 0$					
$l = 1$					
$l = 2$		Table 39	Table 40	Table 41	
$l = 3$				Table 42	
$l = 4$					Table 43

Table 15: Convergence orders for $k = 2, j = 0, l = 1$ with time step $\tau = 10^{-4}$

h	$\ e^n\ $	$Order$	$\ e^n\ $	$Order$
1/4	8.122260e-01		9.918705e-02	
1/8	8.458429e-01	-5.850856e-02	1.024692e-01	-4.696613e-02
1/16	8.547738e-01	-1.515296e-02	1.030492e-01	-8.143834e-03
1/32	8.570361e-01	-3.813233e-03	1.031780e-01	-1.801845e-03

Table 16: Convergence orders for $k = 2, j = 1, l = 1$ with time step $\tau = 10^{-4}$

h	$\ e^n\ $	$Order$	$\ e^n\ $	$Order$
1/4	7.169166e-02		6.189540e-03	
1/8	1.805445e-02	1.989451e+00	7.725189e-04	3.002190e+00
1/16	4.522790e-03	1.997070e+00	9.652195e-05	3.000641e+00
1/32	1.131375e-03	1.999136e+00	1.208548e-05	2.997582e+00

Table 17: Convergence orders for $k = 2, j = 1, l = 2$ with time step $\tau = 10^{-4}$

h	$\ e^n\ $	$Order$	$\ e^n\ $	$Order$
1/4	1.652606e-01		1.071478e-02	
1/8	8.483399e-02	9.620281e-01	2.906554e-03	1.882220e+00
1/16	4.268569e-02	9.908899e-01	7.421362e-04	1.969554e+00
1/32	2.137580e-02	9.977740e-01	1.862606e-04	1.994361e+00

Table 18: Convergence orders for $k = 2, j = 2, l = 2$ with time step $\tau = 10^{-5}$

h	$\ e^n\ $	$Order$	$\ e^n\ $	$Order$
1/4	9.067179e-03		5.671533e-04	
1/8	1.342686e-03	2.755532e+00	3.809727e-05	3.895979e+00
1/16	2.412130e-04	2.476743e+00	2.851774e-06	3.739756e+00
1/32	5.269517e-05	2.194565e+00	2.672112e-07	3.415807e+00

Table 19: Convergence orders for $k = 2, j = 3, l = 3$ with time step $\tau = 10^{-5}$

h	$\ e^n\ $	$Order$	$\ e^n\ $	$Order$
1/4	5.196970e-03		1.247593e-04	
1/8	1.269027e-03	2.033948e+00	1.449317e-05	3.105703e+00
1/16	3.153325e-04	2.008777e+00	1.767677e-06	3.035446e+00
1/32	7.873437e-05	2.001809e+00	2.227589e-07	2.988299e+00

Table 20: Convergence orders for $k = 2, j = 4, l = 4$ with time step $\tau = 10^{-4}$

h	$\ e^n\ $	$Order$	$\ e^n\ $	$Order$
1/4	5.196970e-03		6.863976e-04	
1/8	1.269027e-03	1.974641e+00	8.241034e-05	3.046438e+00
1/16	3.153325e-04	1.993420e+00	1.012732e-05	3.024572e+00
1/32	7.873437e-05	1.998177e+00	1.328450e-06	2.930437e+00

Table 21: Convergence orders for $k = 3, j = 1, l = 2$ with time step $\tau = 10^{-4}$

h	$\ e^n\ $	$Order$	$\ e^n\ $	$Order$
1/4	1.670987e-01		1.040284e-02	
1/8	8.570960e-02	9.631714e-01	2.830643e-03	1.877776e+00
1/16	4.311791e-02	9.911696e-01	7.233917e-04	1.968281e+00
1/32	2.159118e-02	9.978453e-01	1.815894e-04	1.994097e+00

Table 22: Convergence orders for $k = 3, j = 2, l = 2$ with time step $\tau = 10^{-5}$

h	$\ e^n\ $	$Order$	$\ e^n\ $	$Order$
1/4	9.201438e-03		6.734277e-04	
1/8	1.164020e-03	2.982744e+00	4.245300e-05	3.98758e+00
1/16	1.459683e-04	2.995389e+00	2.659047e-06	3.986885e+00
1/32	1.8226353e-05	2.998617e+00	1.733472e-07	3.939173e+00

Table 23: Convergence orders for $k = 3, j = 2, l = 3$ with time step $\tau = 10^{-4}$

h	$\ e^n\ $	$Order$	$\ e^n\ $	$Order$
1/4	2.461944e-02		6.907415e-04	
1/8	6.266297e-03	1.974113e+00	8.841892e-05	2.965719e+00
1/16	1.572490e-03	1.994563e+00	1.106445e-05	2.998423e+00
1/32	3.935074e-04	1.998588e+00	1.452128e-06	2.929691e+00

Table 24: Convergence orders for $k = 3, j = 3, l = 3$ with time step $\tau = 10^{-6}$

h	$\ e^n\ $	$Order$	$\ e^n\ $	$Order$
1/4	8.712987e-04		4.796983e-05	
1/8	6.345320e-05	3.779402e+00	1.581963e-06	4.922340e+00
1/16	5.576660e-06	3.508220e+00	5.637939e-08	4.810404e+00
1/32	6.010600e-07	3.213821e+00	5.462454e-09	3.367547e+00

Table 25: Convergence orders for $k = 3, j = 4, l = 4$ with time step $\tau = 10^{-6}$

h	$\ e^n\ $	$Order$	$\ e^n\ $	$Order$
1/4	4.710535e-04		8.416242e-06	
1/8	5.781054e-05	3.026486e+00	4.870973e-07	4.110894e+00
1/16	7.207176e-06	3.003827e+00	2.990930e-08	4.025544e+00
1/32	9.014070e-07	2.999184e+00	5.234687e-09	2.514419e+00

Table 26: Convergence orders for $k = 4, j = 1, l = 3$ with time step $\tau = 10^{-4}$

h	$\ e^n\ $	$Order$	$\ e^n\ $	$Order$
1/4	2.716178e-01		1.298408e-02	
1/8	1.383182e-01	9.735868e-01	3.455674e-03	1.909705e+00
1/16	6.946239e-02	9.936875e-01	8.782836e-04	1.976208e+00
1/32	3.476853e-02	9.984499e-01	2.202219e-04	1.995729e+00

Table 27: Convergence orders for $k = 4, j = 2, l = 3$ with time step $\tau = 10^{-4}$

h	$\ e^n\ $	$Order$	$\ e^n\ $	$Order$
1/4	2.476214e-02		6.646780e-04	
1/8	6.298864e-03	1.974973e+00	8.522381e-05	2.963327e+00
1/16	1.580428e-03	1.994777e+00	1.067046e-05	2.997635e+00
1/32	3.954779e-04	1.998646e+00	1.405669e-06	2.924293e+00

Table 28: Convergence orders for $k = 4, j = 3, l = 3$ with time step $\tau = 10^{-6}$

h	$\ e^n\ $	$Order$	$\ e^n\ $	$Order$
1/4	9.038281e-04		5.853914e-05	
1/8	5.715505e-05	3.983096e+00	1.849952e-06	4.983842e+00
1/16	3.583032e-06	3.995628e+00	5.818479e-08	4.990701e+00
1/32	2.251702e-07	3.992093e+00	5.232165e-09	3.475162e+00

Table 29: Convergence orders for $k = 4, j = 3, l = 4$ with time step $\tau = 10^{-6}$

h	$\ e^n\ $	$Order$	$\ e^n\ $	$Order$
1/4	2.705839e-03		6.050703e-05	
1/8	3.475762e-04	2.960675e+00	3.841695e-06	3.977288e+00
1/16	4.380892e-05	2.988033e+00	2.399965e-07	4.000658e+000
1/32	5.491110e-06	2.996055e+00	1.574981e-08	3.929607e+00

Table 30: Convergence orders for $k = 4, j = 4, l = 4$ with time step $\tau = 10^{-6}$

h	$\ e^n\ $	$Order$	$\ e^n\ $	$Order$
1/4	7.096378e-05		3.364898e-06	
1/8	2.503060e-06	4.825318e+00	7.897632e-08	5.412998e+00
1/16	1.067160e-07	4.551845e+00	2.586304e-09	4.932456e+00
1/32	2.247061e-08	2.247665e+00	1.980236e-10	3.707147e+00

Table 31: Convergence orders for $k = 2, j = 1, l = 1$ with time step $\tau = 10^{-4}$

h	$\ e^n\ $	$Order$	$\ e^n\ $	$Order$
1/4	2.476214e-02		6.436302e-03	
1/8	6.298864e-03	1.438592e+00	1.118485e-03	2.524686e+00
1/16	1.580428e-03	1.174826e+00	2.386911e-04	2.228330e+00
1/32	3.954779e-04	1.051661e+00	5.674560e-05	2.072564e+00

Table 32: Convergence orders for $k = 2, j = 2, l = 2$ with time step $\tau = 10^{-5}$

h	$\ e^n\ $	$Order$	$\ e^n\ $	$Order$
1/4	9.067179e-03		5.671533e-04	
1/8	1.342686e-03	2.755532e+00	3.809727e-05	3.895979e+00
1/16	2.412130e-04	2.476743e+00	2.851774e-06	3.739756e+00
1/32	5.269517e-05	2.194565e+00	2.672112e-07	3.415807e+00

Table 33: Convergence orders for $k = 2, j = 3, l = 3$ with time step $\tau = 10^{-5}$

h	$\ e^n\ $	$Order$	$\ e^n\ $	$Order$
1/4	5.196970e-03		1.247593e-04	
1/8	1.269027e-03	2.033948e+00	1.449317e-05	3.105703e+00
1/16	3.153325e-04	2.008777e+00	1.767677e-06	3.035446e+00
1/32	7.873437e-05	2.001809e+00	2.227589e-07	2.988299e+00

Table 34: Convergence orders for $k = 2, j = 4, l = 4$ with time step $\tau = 10^{-4}$

h	$\ e^n\ $	$Order$	$\ e^n\ $	$Order$
1/4	5.276425e-02		6.808492e-04	
1/8	1.342498e-02	1.974641e+00	8.241034e-05	3.046438e+00
1/16	3.371586e-03	1.993420e+00	1.012732e-05	3.024572e+00
1/32	8.439626e-04	1.998177e+00	1.328451e-06	2.930436e+00

Table 35: Convergence orders for $k = 3, j = 1, l = 1$ with time step $\tau = 10^{-4}$

h	$\ e^n\ $	$Order$	$\ e^n\ $	$Order$
1/4	1.235269e-01		1.485070e-02	
1/8	4.253941e-02	1.537953e+00	2.061305e-03	2.848901e+00
1/16	1.808968e-02	1.233633e+00	3.432200e-04	2.586353e+00
1/32	8.601552e-03	1.072498e+00	7.111218e-05	2.270965e+00

Table 36: Convergence orders for $k = 3, j = 2, l = 2$ with time step $\tau = 10^{-4}$

h	$\ e^n\ $	$Order$	$\ e^n\ $	$Order$
1/4	1.048823e-02		7.276300e-04	
1/8	1.866607e-03	2.490281e+00	6.014785e-05	3.596620e+00
1/16	4.035579e-04	2.209570e+00	6.163514e-06	3.286688e+00
1/32	9.652462e-05	2.063807e+00	8.686333e-07	2.826934e+00

Table 37: Convergence orders for $k = 3, j = 3, l = 3$ with time step $\tau = 10^{-6}$

h	$\ e^n\ $	$Order$	$\ e^n\ $	$Order$
1/4	8.712987e-04		4.796983e-05	
1/8	6.345320e-05	3.779402e+00	1.581963e-06	4.922340e+00
1/16	5.576661e-06	3.508220e+00	5.637940e-08	4.810404e+00
1/32	6.010604e-07	3.213820e+00	5.462806e-09	3.367454e+00

Table 38: Convergence orders for $k = 3, j = 4, l = 4$ with time step $\tau = 10^{-6}$

h	$\ e^n\ $	$Order$	$\ e^n\ $	$Order$
1/4	4.710535e-04		8.416242e-06	
1/8	5.781054e-05	3.026486e+00	4.870973e-07	4.110894e+00
1/16	7.207176e-06	3.003827e+00	2.990930e-08	4.025544e+00
1/32	9.014071e-07	2.999183e+00	5.234441e-09	2.514487e+00

Table 39: Convergence orders for $k = 4, j = 1, l = 2$ with time step $\tau = 10^{-4}$

h	$\ e^n\ $	$Order$	$\ e^n\ $	$Order$
1/4	1.680932e-01		1.019948e-02	
1/8	8.606377e-02	9.657835e-01	2.813409e-03	1.858104e+00
1/16	4.329160e-02	9.913190e-01	7.223234e-04	1.961603e+00
1/32	2.167803e-02	9.978530e-01	1.815416e-04	1.992344e+00

Table 40: Convergence orders for $k = 4, j = 2, l = 2$ with time step $\tau = 10^{-4}$

h	$\ e^n\ $	$Order$	$\ e^n\ $	$Order$
1/4	1.659611e-02		1.913745e-03	
1/8	2.746179e-03	2.595348e+00	1.336710e-04	3.839640e+00
1/16	5.644401e-04	2.282533e+00	1.117750e-05	3.580018e+00
1/32	1.323725e-04	2.092217e+00	1.258791e-06	3.150486e+00

Table 41: Convergence orders for $k = 4, j = 3, l = 2$ with time step $\tau = 10^{-4}$

h	$\ e^n\ $	$Order$	$\ e^n\ $	$Order$
1/4	1.475717e-02		1.880159e-03	
1/8	1.839962e-03	3.003668e+00	1.154356e-04	4.025694e+00
1/16	2.298950e-04	3.000629e+00	7.199269e-06	4.003094e+00
1/32	2.881565e-05	2.996050e+00	6.649049e-07	3.436630e+00

Table 42: Convergence orders for $k = 4, j = 3, l = 3$ with time step $\tau = 10^{-6}$

h	$\ e^n\ $	$Order$	$\ e^n\ $	$Order$
1/4	1.036100e-03		6.412737e-05	
1/8	9.113811e-05	3.506965e+00	2.618642e-06	4.614049e+00
1/16	9.779329e-06	3.220247e+00	1.323056e-07	4.306873e+00
1/32	1.166344e-06	3.067742e+00	9.121470e-09	3.858464e+00

Table 43: Convergence orders for $k = 4, j = 4, l = 4$ with time step $\tau = 10^{-6}$

h	$\ e^n\ $	$Order$	$\ e^n\ $	$Order$
1/4	7.096379e-05		3.3648980e-06	
1/8	2.503069e-06	4.825313e+00	7.895302e-08	5.412998e+00
1/16	1.067212e-07	4.551780e+00	2.582612e-09	4.934091e+00
1/32	2.247073e-08	2.247728e+00	1.988624e-10	3.698988e+00